Electronic Theses and Dissertations

Theses, Dissertations, and Major Papers

1-1-2000

Effects of humidity on the adsorption of coating solvent (m-xylene) on activated carbon.

Sukanta Basu
University of Windsor

Follow this and additional works at: https://scholar.uwindsor.ca/etd

INFORMATION TO USERS

This manuscript has been reproduced from the microfilm master. UMI films the text directly from the original or copy submitted. Thus, some thesis and dissertation copies are in typewriter face, while others may be from any type of computer printer.

The quality of this reproduction is dependent upon the quality of the copy submitted. Broken or indistinct print, colored or poor quality illustrations and photographs, print bleedthrough, substandard margins, and improper alignment can adversely affect reproduction.

In the unlikely event that the author did not send UMI a complete manuscript and there are missing pages, these will be noted. Also, if unauthorized copyright material had to be removed, a note will indicate the deletion.

Oversize materials (e.g., maps, drawings, charts) are reproduced by sectioning the original, beginning at the upper left-hand corner and continuing from left to right in equal sections with small overlaps.

Photographs included in the original manuscript have been reproduced xerographically in this copy. Higher quality 6" x 9" black and white photographic prints are available for any photographs or illustrations appearing in this copy for an additional charge. Contact UMI directly to order.

ProQuest Information and Learning
300 North Zeeb Road, Ann Arbor, MI 48106-1346 USA
800-521-0600

UMI®

EFFECTS OF HUMIDITY ON THE ADSORPTION OF COATING SOLVENT (m-XYLENE) ON ACTIVATED CARBON

by

Sukanta Basu

A Thesis
Submitted to the College of Graduate Studies and Research
through Civil and Environmental Engineering
in Partial Fulfilment of the Requirements for
the Degree of Master of Applied Science at the
University of Windsor

Windsor, Ontario, Canada
2000

© 2000 Sukanta Basu

The author has granted a non-exclusive licence allowing the National Library of Canada to reproduce, loan, distribute or sell copies of this thesis in microform, paper or electronic formats.

The author retains ownership of the copyright in this thesis. Neither the thesis nor substantial extracts from it may be printed or otherwise reproduced without the author's permission.

L'auteur a accordé une licence non exclusive permettant à la Bibliothèque nationale du Canada de reproduire, prêter, distribuer ou vendre des copies de cette thèse sous la forme de microfiche/film, de reproduction sur papier ou sur format électronique.
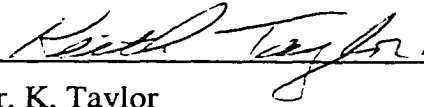
L'auteur conserve la propriété du droit d'auteur qui protège cette thèse. Ni la thèse ni des extraits substantiels de celle-ci ne doivent être imprimés ou autrement reproduits sans son autorisation.

0-612-62186-3

Canadä

919585

APPROVED BY:

Dr. K. Taylor
Chemistry and Biochemistry

Dr. R. L. Arndt
Civil and Environmental Engineering

Dr. P. F. Henshaw, Co-advisor
Civil and Environmental Engineering

Dr. N. Biswas, Co-advisor
Civil and Environmental Engineering

Dr. J. K. Bewtra, Chair
Civil and Environmental Engineering

ABSTRACT

Control of coating solvent vapors by adsorption on activated carbon in the automotive industry can be affected by the presence of humidity. As a foundation to better understand the adsorptive behavior of these organic solvents, in this investigation, adsorption of m-xylene in the presence of water vapor on granular activated carbon was studied.

Single component (m-xylene and water vapor) adsorption experiments were first conducted as prerequisites for the binary component (m-xylene with water vapor) studies. The dynamic method of gas adsorption techn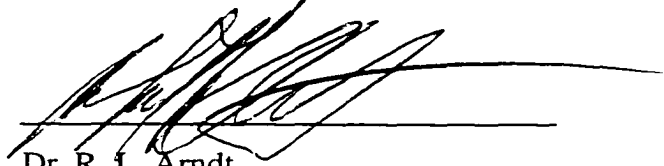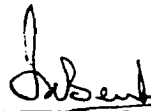ique (passing a flux composed of carrier gas and adsorbate vapor through a fixed bed adsorbent and subsequently analyzing the outlet adsorbate concentrations) was used throughout this research. The experimental results were then compared with predictive models to capture the dominant features of the data.

For the equilibrium and kinetic studies of water vapor adsorption, an online digital hygrometer was used in conjunction with an electronic balance. Relative humidity values from 18 to 96% were examined. The adsorption isotherm was found to resemble a type V isotherm (Brunauer classification system). The adsorption capacities from the gravimetric measurement were within 14% of the values obtained from the kinetic studies based on the area integration of the breakthrough curves.

The m-xylene adsorption system design was similar to the water vapor adsorption system, except the online measurement of the adsorbate was done by gas chromatograph with the help of a six-port valve. The concentration range studied was 52 to 1030 ppm. The limiting pore volumes resulting from the m-xylene adsorption experiments (0.56 mL/g)

iii

differed considerably from those found in the water vapor adsorption studies (0.2 mL/g). The explanation of this anomalous behavior was beyond the scope of this study.

A conglomeration of the single component systems was employed for the binary component adsorption experiments. Relative humidity values of 54 to 88% and organic concentrations from 178 to 1120 ppm were studied. A surface plot and a matrix table were used to interpret the complicated binary data. The adsorption capacity of m-xylene decreased with increasing relative humidity. The effect of humidity was greater at low m-xylene concentrations.

To My Family

v

ACKNOWLEDGEMENTS

I wish to express my deep sense of gratitude to Dr. Paul Henshaw for his extraordinary support and guidance at all stages throughout this study, especially for all the "5 minutes discussion sessions" [never less than an hour] he granted me.

I would like to sincerely thank Dr. Nihar Biswas for his priceless advice regarding my research, and for having provided the facilities needed for this work.

The quality of this thesis was also significantly improved by the valuable suggestions of my other committee members, Dr. Richard Arndt, Dr. Keith Taylor and Dr. Jatinder Bewtra, which I greatly appreciated.

The technical support I received from Mr. Steve Budinsky of Technical Support Centre, and Mr. Patrick Seaguin, technician, Civil and Environmental Engineering was of great importance and it certainly saved me a lot of time!

Thanks to all my friends in Civil and Environmental Engineering, including a special thought to Mr. Ahmed Elgendy for his generous help during my research. Most of all, I am indebted to my friend Valérie Guérin, for being there, with me, in the course of many happy and difficult times.

Lastly, I am grateful to the Civil and Environmental Engineering program for the financial support I received throughout my graduate study at University of Windsor.

TABLE OF CONTENTS

CHAPTER THREE – MATERIALS AND METHODS

CHAPTER FOUR – RESULTS AND DISCUSSION

CHAPTER FIVE – CONCLUSIONS AND RECOMMENDATIONS

---

* To enhance the readability of this thesis the terms in *italics* are defined in the glossary.

NOTATIONS

A wide range of notations has been employed in this thesis. To make reference to the original papers easier, the original notations have been retained.

a	adsorption capacity (g/g)
A	differential molar work of adsorption (cal/mole)
a_0	number of primary adsorption center
a_c	constant of equation 2.9
a_s	limiting adsorption capacity (g/g)
b	kinetic constant in equation 2.12
c	constant in equation 2.3
C_0	inlet concentration (ppm)
C_x	outlet concentration (ppm)
f	constant in equation 2.14
h	relative humidity (%)
h_0	hysteresis
k	kinetic constant in equation 2.13 (min^{-1})
k_1	rate of desorption (equation 2.1)
k_2	rate of adsorption (equation 2.1)
k_3	empirical factor in equations 2.4, 2.5 and 2.6
k_4	constant in equation 2.21
k_v	adsorption rate constant in equation 3.1

x

K	empirical constant in equation 2.11
K_F	constant in equation 2.14
M_e	adsorbate uptake at equilibrium (g/g)
M_t	adsorbate uptake at time t (g/g)
p	equilibrium vapor pressure of adsorbate (kPa)
p_s	saturated vapor pressure (kPa)
P	equilibrium vapor pressure of adsorbate (kPa)
P_0	saturated vapor pressure (kPa)
P_{50}	empirical constant in equation 2.11
P_s	saturated vapor pressure (kPa)
q	adsorption capacity (g/g)
Q	air flow rate (L/min)
q_0	limiting adsorption capacity (g/g)
q_{VOC}	VOC adsorption capacity (g/g)
$q_{VOC,RH=0}$	pure component VOC adsorption capacity (g/g)
n	constant in equation 2.21
R	gas constant (1.987 cal/mole °K)
RH	relative humidity (%)
t	time (min)
T	absolute temperature (°K)
t_B	breakthrough time (min)
V_0	limiting pore volume of the adsorbent (cc/g)
V_0	molar volume of organic in equations 2.19 and 2.20 (cc/gmol)

V_w	molar volume of water in equations 2.19 and 2.20
W	volume of organic adsorbate adsorbed (cc/g)
W_0	limiting adsorption volume (cc/g)
W_e	limiting adsorption capacity (g/g)
ΔW	water uptake or loss (g/g)

GREEK LETTERS

α	difference between two points on isotherm (equation 2.12)
β	constant of equations 2.10 and 2.16
γ	constant of equation 2.10
ε	adsorption potential (cal/mole)
κ	DR equation constant (equation 2.16)
ρ	density of adsorbate (g/cc)
ρ_B	bulk density of carbon (g/cc)

ACRONYMS

ASTM	The American Society for Testing and Materials
CAA	Clean Air Act
CAAA	Clean Air Act Amendments
CCME	Canadian Council of Ministers of the Environment
CCOHS	Canadian centre for Occupational Health and Safety
FID	Flame Ionization Detector
GAC	Granular Activated Carbon
GC	Gas Chromatography
HAP	Hazardous Air Pollutant
HPLC	High-Performance Liquid Chromatography
IGA	Intelligent Gravimetric Analyzer
NAAQS	National Ambient Air Quality Standard
NOx	Nitrous Oxides
OEM	Original Equipment Manufacturers
PPM	Parts Per Million (by Volume)
RACT	Reasonably Available Control Technology
RH	Relative Humidity
THF	Tetrahydrofuran
UV	Ultra Violet
VOC	Volatile Organic Compound

LIST OF TABLES

LIST OF ILLUSTRATIONS

CHAPTER ONE

INTRODUCTION

1.1   BACKGROUND

Coating of parts by priming, painting and scaling is the most expensive unit operation in automobile manufacturing and its major source of environmental pollution in terms of *volatile organic compounds* (VOCs), *hazardous air pollutants* (HAPs), waste paint streams and solid waste. It consumes a disproportionate amount of energy considering the small amount of paint involved. Today, the complete automobile painting process requires approximately 16% of the total primary energy consumption for the entire vehicle production process, depending on the car's size (Harsch et al. 1999). According to Ford Motor Company's 1997 U.S. Toxic Release Inventory Data, approximately 80% of all pollutants that were released to air, water and land from all Ford U.S. automotive operations in 1997 were from paint solvents (Kim et al. 2000). In 1992, General Motor's annual pollution control costs were over $150 million for the U.S automotive operations. Although, the pollution control costs were insignificant compared to General Motor's annual operational costs, more than 60% of these costs were devoted to air emissions control (Geffen et al. 1998).

Clearly, the above figures depict the economic and environmental importance of the painting process in the automotive industry.

1.2   PAINT SOLVENTS AND AIR POLLUTION

Traditional organic automotive paint solvents (Table A.1, Appendix A), nearly all of which are categorized as VOCs, have dominated the surface coating process for decades (Healey et al. 1998).

The organic solvents perform the critical role of transporting the resins, pigments, stabilizers and extenders and giving the coating the necessary viscosity, surface tension and other chemical properties that aid in the consistent application of individual coating layers. The choice of a particular organic solvent depends on the substrate composition and geometry, application equipment to be used, curing temperature and time range, and coating solids' characteristics.

Evaporation during drying of the paint solvents is the major source of VOC emissions in automotive manufacturing. Additionally cleaning, priming, surfacing, repairing and equipment cleaning, also contribute to the overall VOC emissions from the automotive painting process.

1.3   REGULATIONS

VOCs play the role of precursors in the photochemical smog pollution. When VOCs are mixed with nitrogen oxides (NO_x) and irradiated by ultraviolet (UV) light, a complex chain of reactions converts them into ozone, aldehydes, hydrogen peroxide, peroxyacetyl nitrate, organic and inorganic acids and fine particles. Among these, ozone is considered to be the most significant photochemical pollutant because of its wide range of effects on human health, plant growth and climatic change (Bloemen et al. 1993). To achieve ground level ozone reduction, regulations principally focus on the reduction of VOCs emissions. In

2

the United States, the Clean Air Act (CAA) is one of the numerous statutes and regulations that regulate VOCs emissions.

But after more than 20 years of regulations, approximately 100 urban areas in the United States still exceed the ozone National Ambient Air Quality Standards (NAAQS), referred to as *ozone nonattainment areas*. The Clean Air Act Amendments (CAAA) of 1990 greatly increased the regulatory framework for control of volatile organic compound emissions. The amendments require that each state with one or more ozone nonattainment areas impose controls on sources of VOCs sufficient to allow those areas to comply with the ambient standard (Hellwig 1998). As a result of the CAAA, many original equipment manufacturers (OEMs) were being forced to reduce VOC emissions in their painting operations (Triplett 1995b).

In addition, in July 1997, the Environmental Protection Agency (EPA) issued its final ruling to reduce the NAAQS for ozone from 0.12 ppm to 0.8 ppm averaged over an 8-hour period (Hussey et al. 1998). This greatly increased the number of nonattainment areas. As a result, many minor sources of VOC emissions became significant. Facilities that previously were subject only to either state VOC emissions regulations or were exempt from regulation were then forced to implement federally defined Reasonably Available Control Technologies (RACTs).

Regulations regarding VOC emissions in general or specific organic compounds are currently found in several jurisdictions in Canada (Rix 1998). In 1990, The Canadian Council of Ministers of the Environment (CCME) introduced a NO_x/VOCs Management Plan (CCME, 1990). Apart from that, a number of studies have been conducted through the CCME, leading to the development of Codes of Practice for different industries, such as the

3

New Source Performance Standards and Guidelines for the Reduction of Volatile Organic Compound Emissions from Canadian Automotive OEM Coating Facilities (CCME, 1995). Source Performance Standards Limits (SPSLs) are expressed in grams of VOC emitted per square metre of total vehicle body surface area. Separate limits exist for automobiles, passenger vans and sport/utility vehicles, light duty trucks and vans. Table 1.1 shows the Source Guideline Limits.

Table 1.1. Source Guideline Limits

	Interim*	Final**
Automobiles	65 gm/m^2	55 gm/m^2
Passenger vans & sport/utility vehicles	70 gm/m^2	60 gm/m^2
Light duty trucks & vans	80 gm/m^2	75 gm/m^2

* Interim limits take effect on January 1, 2000
** Final limits take effect on January 1, 2005
Source: Mancina, A. S. (1998)

1.4   EMISSIONS REDUCTION OPTIONS

For automotive coating operations, effectively meeting today's strict VOC regulations is an ongoing challenge. Three primary alternatives may be explored to achieve this goal.

The first is to switch to "environmentally friendly" coatings, such as waterbornes, UV-cure or powder coatings. But often the critical requirements of high gloss, smooth surface and minimal first-run defects now met by solventborne clear coats are not fulfilled by these coatings.

The second option is to reduce the VOC emission rate through changes to the paint-line design. For example, paint-booth exhaust volumes can be reduced through air re-circulation (Triplett 1995a).

4

The final alternative is to install add-on controls. This is the solution chosen by most automotive companies today. Several options are available to control VOCs: oxidation, *adsorption*, UV/ozone catalytic oxidation, biofilters, and wet/dry filtration etc. Tables 1.2 and 1.3 compare the total annualized costs and cost effectiveness of some of these abatement technologies. To compare the technologies on a common basis, the costs were calculated using published values and vendor supplied cost factors on four model gas streams (100 and 10 ppm benzene in air and 100 and 10 ppm tetrachloroethylene in air, all at a flow rate of 10,000 scfm) (EPA 1995).

Table 1.2 Total Annualized Costs ($/Year)

Processes	Benzene Conc. (ppm)		Tetrachloroehylene Conc. (ppm)	
	100	10	100	10
Catalytic Incineration	271,923	274,376	290,705	291,393
Regenerative Thermal Incineration	180,991	180,991	245,916	252,316
Regenerable Fixed Bed Carbon Adsorption	98,873	98,873	98,199	58,711
QVF Absorption	331,400	331,400	331,400	331,400

Source: EPA (1995)

Table 1.3 Cost Effectiveness ($/Ton VOC Removed)

Processes	Benzene Conc. (ppm)		Tetrachloroehylene Conc. (ppm)	
	100	10	100	10
Catalytic Incineration	5,489	55,381	5,868	58,829
Regenerative Thermal Incineration	3,653	38,147	4,964	50,928
Regenerable Fixed Bed Carbon Adsorption	1,996	1,996	1,780	11,850
QVF Absorption	6,700	66,900	3,300	32,800

Source: EPA (1995)

Controlling VOC emissions from spray coating operations has historically been cost prohibitive, due to high exhaust flow rates coupled with low VOC concentrations (approximately 100 parts per million by volume) (Ayer 1997, Kim 1997).

One way of compensating for the high control costs is by the recovery of the VOCs. Low cost *adsorbent* (*activated carbon*), high capture efficiency (in the range of 95-98%) and economical recovery established adsorption as the technology of choice (Ruhl 1993 and Basu et al. 2000).

1.5   CONTROL OPTION — ADSORPTION

However, the adoption of adsorption technology is not straightforward (Golovoy 1981). Rational methods are essential for reliable and economically effective design and operation of an adsorption system. Conscious choice of process factors (e.g. proper adsorbent) can reduce the spray booth exhaust concentration by a factor of 10 in surface coating operations (Hussey et al. 1998).

1.6   ADSORPTION—EFFECTS OF HUMIDITY

Activated carbon's adsorptive capacity drops significantly in the presence of humidity (Werner et al. 1986). In the case of spray booths with wet Venturi scrubbers (widely used in automotive coating facilities for primary removal of particulate matter followed by adsorption beds), the humidity level of the inlet stream to the adsorbent bed is generally very high. The contaminant stream may be heated to reduce the relative humidity but the increase in temperature usually reduces the adsorption efficiency. In applications like steam regeneration of activated carbon, adsorption of water vapor also has been encountered.

6

Residual water present on the carbon after regeneration affects the performance of the subsequent adsorption step. Moreover, in recent years, there has been a growing interest in the application of waterborne coatings. In waterborne coatings organic solvents are replaced with water, thus reducing VOC emissions significantly (but not completely) while unfortunately increasing the humidity level in the spray booth.

Since some level of humidity will always be present in spray booths, there is a need for a better understanding of the adsorptive behavior of VOCs in the presence of humidity on activated carbon.

1.7 OBJECTIVE

The objective of this research was to study the adsorption of an automotive coating solvent in the presence of water vapor on activated carbon.

1.8 SCOPE

To study the interference of humidity with the adsorption of organic solvent (VOC), it was essential to understand the manner in which water and VOC adsorb onto activated carbon individually. So, both binary component (m-xylene with water) and single component (Water and m-xylene) adsorption experiments were conducted using a laboratory activated carbon column. Several predictive models were also investigated for their capability to model the adsorption processes and experimental results were compared with the model predictions wherever possible.

7

The selection of the solvent (m-xylene) was based on its major usage as a paint solvent (Table A.2, Appendix A and Golovoy 1981) as well as its posing a threat to the public, workers and the environment (Bloemen et al. 1993 and CCOHS 1984).

In essence the scope of this work was to:

- study the equilibria and kinetics of water vapor adsorption onto granular activated carbon (GAC).

- study the single component VOC adsorption onto GAC.

- demonstrate the adverse effect of humidity on VOC adsorption.

- compare the theoretical models delineating the above processes.

8

CHAPTER TWO

LITERATURE REVIEW

2.1   WATER VAPOR ADSORPTION

Water has a complicated sorptive behavior as revealed by its characteristic sigmoid-shaped isotherm (Type V in the *Brunauer classification system*). This S-shape indicates that more than one mechanism is responsible for the adsorption of water vapor onto *microporous* activated carbon (Noll et al. 1991). Adsorption of water vapor begins on the primary adsorption sites (oxygen surface complexes) at low relative humidities (Dubinin 1980). The number of such available primary sites decreases with increasing relative humidities (RH) as more water vapor adsorbs onto those sites (Qi et al. 2000). The adsorbed water molecules then act as secondary adsorption sites and other water molecules attach to these by hydrogen bonding. At a sufficiently high relative humidity, *capillary condensation* occurs to fill the micropores with water, causing a sharp increase in the adsorption capacity. This phenomenon apparently begins to occur at approximately 50% relative humidity, depending on the type of carbon (Werner et al. 1988).

2.1.1   Water Vapor Adsorption: Adsorption Equilibria

Accurate estimation of adsorption equilibria is of great importance when dealing with experimental studies and the development of models that predict the performance of adsorbers (Huggahalli et al. 1996). But, due to the unique sigmoidal behavior caused by the primary and secondary adsorption sites, only a few adsorption isotherm models can be used to describe the adsorption equilibria of water vapor onto activated carbon (Qi et al. 2000).

9

The first attempt at an approximate quantitative description of the initial region of the water vapor adsorption isotherm (DS-1) on carbonaceous adsorbents was made by Dubinin and Serpinsky (Dubinin 1980). Development of the adsorption isotherm equation began with the assumption of a dynamic equilibrium between adsorption and desorption (Equation 2.1). If a_0 is the number of primary adsorption centers, and a is the adsorption value for relative humidity of $h = p/p_s$, then the dynamic equilibrium condition will be expressed by:

$$k_2(a_0 + a)h = k_1 a \tag{2.1}$$

The corresponding adsorption isotherm equation (DS-1) becomes:

$$a = \frac{a_0 ch}{(1 - ch)} \tag{2.2}$$

$$\text{where, } c = \frac{k_2}{k_1}$$

Equation 2.2 describes the initial region and the main part of the sharp rise of the isotherm up to $h < 1/c$. The equation parameters a_0 and c can be easily determined graphically from the linear form of the equation:

$$\frac{h}{a} = \frac{1}{(a_0 c)} - \frac{h}{a_0} \tag{2.3}$$

The DS-1 model is only valid for RH < 60% (Qi et al. 2000).

Dubinin et al. (1981) extended their earlier model (DS-1) to describe the adsorption of water vapor over the entire pressure range. An empirical factor $(1-k_3 a)$ was introduced into the dynamic equilibrium equation to take into account the decrease in the number of acting adsorption centers with an increase in filling.

10

The dynamic equilibrium condition was expressed by:

$$k_2(a_0 + a)(1 - k_3 a)h = k_1 a \qquad (2.4)$$

The parameter k was determined from the condition $a = a_s$ at $h=1$. Where, a_s is the limiting value of vapor adsorption. Denoting the kinetic constant ratio $c = k_2/k_1$, the expression for k_3 becomes:

$$k_3 = \frac{1}{a_s} - \frac{1}{[c(a_0 + a_s)]} \qquad (2.5)$$

As a result the isotherm equation (DS-2) for water vapor adsorption on active carbon takes the form (Barton et al. 1991):

$$\frac{a}{h} = c(a_0 + a)(1 - k_3 a) \qquad (2.6)$$

The parameters (a_0, c, k_3) of this equation can be determined from a single adsorption isotherm (Dubinin et al. 1981).

Barton et al. (1991) modified the models of Dubinin et al. (1980, 1981) and applied them to water vapor adsorption on a number of carbons having a wide variation in surface oxide concentration. Following Dubinin and Serpinsky, they derived the cubic form of the DS model (DS-3). The model assumes that water vapor adsorption takes place initially on very active primary sites on the carbon surface. The concentration of these sites is s_0. The adsorption of water on these sites is similarly expressed as a_0. Secondary, hydrogen bonded water is designated as a_H. Assuming the adsorption equilibrium is described by the mass action law, the following can be written:

$$c_1(s_0 - a_0)h + (c_2 a_0 + c_3 a_H)(1 - ka^2)h = c_4 a_0 + c_5 a_H \qquad (2.7)$$

c_1-c_5 are kinetic parameters governing the rates of adsorption and desorption.

11

The empirical factor $(1-ka^2)$ is introduced to cause a decrease in adsorption site concentration as total adsorption (a) increases. Following certain assumptions and after some simplification and rearrangement, Equation 2.7 (DS-3) becomes:

$$h = \frac{1}{c[1 - ka(a_0 + a)]} \qquad (2.8)$$

The parameter, k, is connected with the saturated adsorption (similar to DS-2), a_s, when h=1. But, DS-3 is unsuitable for modeling, because it can not be inverted to describe the dependence of adsorption capacity on the relative humidity (Huggahalli et al. 1996).

Barton et al. (1992) introduced a fourth parameter (a_c) in the model DS-3 to provide better representation for super activated carbon (AX-21) and largely microporous char (PVDC). The new equation (DS-4) suggested:

$$h = \frac{a}{ca_0 + ca\left[1 - \exp\left(-k^2(a - a_c)^2\right)\right]} \qquad (2.9)$$

The values of the parameters a_0, c, k and a_c were obtained, as before, by non-linear regression analysis of experimental data. The DS-4 model provided excellent fit for AX-21 and PVDC char as well as for the *BPL* carbons (Barton et al. 1992).

Kisarov (1984) obtained an isotherm equation by treating adsorbent-*adsorbate* and adsorbate-adsorbate interactions as quasi-chemical reactions. But, evaluation of the parameters in the resultant expression is indirect and cumbersome (Huggahalli et al. 1996).

Doong and Yang (1987) modified the original Dubinin-Radushkevich (DR) equation (Dubinin 1975) by including two additional parameters (hysteresis, h_0, and activity coefficient, γ) to advance the quantitative description of water vapor adsorption (Qi et al. 2000).

12

The DY model was written as follows (Qi et al. 2000):

$$q = \rho V_0 \exp\left\{ -\left(\frac{T}{\beta E}\right)^2 \left(\ln\frac{\gamma P_0}{P}\right)^2 - (\ln h_0)^2 \right\} \qquad (2.10)$$

Where, q = adsorption capacity of water vapor; ρ = density of adsorbed water; V_0 = limiting pore volume of the adsorbent; P = vapor pressure of water; P_0 = saturation vapor pressure of water; T = absolute temperature; β and E are DR isotherm parameters; γ = coefficient to account for different degrees of association in the liquid and adsorbed phases; and h_0 accounts for hysteresis. The value for γ (RH < 60%) is calculated using the Dubinin-Serpinsky equation (DS-2), whereas γ (RH > 60%) = 1 (Doong et al. 1987).

Recently, Qi et al. (1998) developed the QHR model (Equation 2.11) and compared it with the DY model (Qi et al. 2000). The QHR model was shown to be in better agreement with experimental water vapor adsorption data than the DY model for a predominantly microporous coal-based activated carbon (Qi et al. 2000). The QHR isotherm model can be written as (Qi et al. 1998):

$$q = \frac{\rho V_0}{1 + \exp\left[K\left(\frac{P_{50}}{P_0} - \frac{P}{P_0}\right)\right]} \qquad (2.11)$$

Where, q, ρ, V_0, P, P_0 are same as described above. The empirical parameters P_{50}, and K are derived by fitting the experimental data to the model. The model was also verified using experimental data for water vapor adsorption onto four different activated carbon adsorbents from 288 to 308 K at 101 kPa total pressure (Qi et al. 1998).

13

Hassan et al. (1991) compared the water vapor adsorption data (on BPL activated carbon) of Freeman et al. (1979), Barton et al. (1984), Mahle et al. (1988) and Hassan et al. (1991). Figure 2.1 exhibits the characteristic sigmoid shape water vapor adsorption isotherm. Hassan et al. (1991) attributed the large differences in the uptake values (as shown in the figure) to differences in the regeneration temperature, lots of activated carbon used and the ultimate vacuum attainable in each system during regeneration.
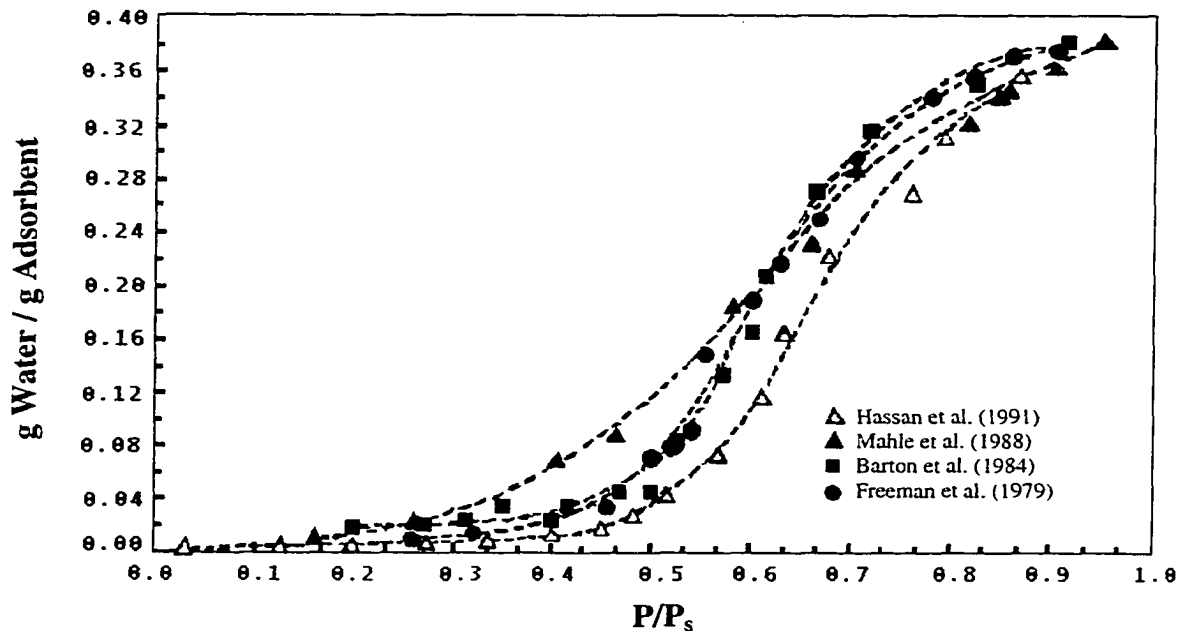
Figure 2.1. Comparison of Water Vapor Adsorption Isotherms at 298 K

(*Source:* Hassan et al. 1991)

2.1.2   Water Vapor Adsorption: Kinetics

For the water vapor adsorption, knowledge of the shape of the *breakthrough curve* is also desirable. The time to breakthrough is often the criterion used to assess the performance of an activated carbon unit. But, investigations of the adsorption kinetics of water vapor on activated carbons are very scarce (Foley et al. 1997).

14

Lin et al. (1996) investigated the relationship between adsorption/desorption kinetics and equilibrium partitioning of water vapor on activated carbon grains. The adsorption and desorption isotherms, and adsorption and desorption kinetic curves were measured by an electrobalance (RH 0 to 86%) at 20°C. A model that accounts for transport within grains by pore and surface diffusion was coupled with the experimentally determined piecewise-linear isotherm to interpret the experimental kinetic data. The model results indicated that gas-phase diffusion dominates transport through the pores at RH ≤ 60%. *Surface diffusion* was found to be important at higher RH values.

Lodewyckx et al. (1997) reported a general formula for the dynamic uptake of water on microporous activated carbons. Three different types of commercial activated carbons (Chemviron BPL, SC II and Norit R1E) were equilibrated at a known relative humidity (0 to 90%). Then they were exposed to an air flow with a different (higher or lower) relative humidity. The samples were weighed at regular intervals to obtain a curve for weight loss/gain vs. time. This curve was fitted with the Equation 2.12 using non-linear regression.

$$\Delta W = \alpha \left(1 - \exp\left(-\frac{bt}{\sqrt{|\alpha|}} \right) \right) \tag{2.12}$$

Where, ΔW = water uptake or loss; α = difference between the two points on the water isotherm; b = kinetic constant and t = time.

In a later work Lodewyckx et al. (1998) tested the validity of Equation 2.12 for two other types of commercial activated carbon (Chemviron ASC-T and Norit C Granular). They also tried to evaluate the influence of different parameters (temperature, air flow and bed depth) on the kinetic constant b.

15

Foley et al. (1997) studied the adsorption of water vapor on a highly microporous carbon derived from the carbonization of coconut shell. The static atmosphere water vapor adsorption/desorption kinetics for a carbon with preadsorbed water were studied using an Intelligent Gravimetric Analyzer (IGA) for a series of changes in vapor pressure. The adsorption rate constants were also studied for three relative humidities for a dynamic flow system at a constant temperature. The water uptake was described by the following phenomenological model:

$$\frac{M_t}{M_e} = 1 - \exp\left(-kt\right) \tag{2.13}$$

Where, M_t = gas uptake at time t, M_e = gas uptake at equilibrium, t = time and k = empirical constant.

The rate constants were calculated from the gradient of the $\ln(1-M_t/M_e)$ versus time graph. The rates of adsorption and desorption vary with the position on the isotherm and hence the mechanism of the adsorption process. The fastest rates were observed for adsorption on the primary adsorption centers at low relative pressures. The slowest rates of both adsorption and desorption were observed in the region of relative humidities in the range 40-70%, where the adsorption process involves the growth of clusters of water molecules on the primary adsorption centers. This leads to water molecules bridging between pore walls and adjacent water molecule clusters when a significant amount of free surface is available and eventually leads to condensation of water vapor in the pores.

2.2 VOC ADSORPTION

The mechanism of the VOC adsorption is different from that of water vapor adsorption. Hydrogen bonding to the oxidized adsorption sites is the major influence during water vapor adsorption, whereas *dispersional forces* greatly influence the adsorption of VOCs. Thus, volume filling of the micropores occurs with organic vapor, while adsorption of water begins at specific sites on the carbon surfaces (Werner et al. 1988).

There have been numerous investigations on the adsorption isotherms of VOCs on activated carbons. A great number of isotherm models also have been developed. Werner et al. (1988) made an excellent review of the VOC adsorption predictive models. In the following section two of the most successful models (Freundlich isotherm and Potential theory of adsorption) will be briefly presented.

2.2.1 Prediction of VOC Adsorption Capacity

Freundlich isotherm is an empirical equation (Equation 2.14) whose form is simply designed to fit the parabolic shape of a typical adsorption isotherm (Werner et al. 1988).

$$W = K_F P^f \qquad (2.14)$$

Where, W = volume of organic adsorbate adsorbed, P = partial pressure of the adsorbate and K_F and f are empirical coefficients (unique for each adsorbate-adsorbent pair and operating condition). For the design of adsorption systems, the equilibrium adsorption study on the same adsorbent at different operating conditions is considered as an essential part of the design. The Freundlich equation, however, is operating condition specific and can not be used as a predictive model for untested adsorbates.

17

The Potential theory of adsorption (Noll et al. 1991, Werner et al. 1988) or the theory of volume filling (Dubinin et al., 1971; Dubinin 1975) is based on rational physical and chemical concepts rather than on the empirical fit of experimental data. This theory is specifically applicable to the adsorption of organic vapors on microporous adsorbents (e.g. activated carbon). This model predicts, in principle, the adsorption capacity of a given adsorbent for any untested adsorbate at any concentration and at any temperature.

Based on the Potential theory of adsorption, originally developed by Polanyi (1932), Dubinin in 1960 developed the theory of adsorption in micropores (Dubinin 1975). The central idea was the concept of adsorption potential involving adsorbent and adsorbate. Adsorption potential was defined as the work to transfer an adsorbate molecule from the vapor phase to a compressed state within the pores of the carbon. Mathematically, the adsorption potential (ε) can be expressed as:

$$\varepsilon = RT\ln\left(\frac{P_s}{P}\right) \tag{2.15}$$

Where, R = universal gas constant, T = absolute temperature, P = equilibrium vapor pressure of the adsorbate vapor at a given temperature, and P_s = saturation value of P.

The potential was conceptualized (Figure 2.2) as a field extending outward from the surface of the carbon and decreasing in force with increasing distance from the surface. The value of ε varies within the adsorption space from some maximum value (ε_{max}) to zero, depending upon proximity to the adsorbent surface (Tien 1994). W is the volume of space in the carbon pores in which the potential compressional forces are greater than or equal to the corresponding ε value. Therefore, W_0 (corresponding to $\varepsilon = 0$) is the limiting adsorption volume of the microporous carbon. At the surface of the carbon, $W = 0$ ($\varepsilon = \varepsilon_{max}$).

18

At equilibrium the adsorbed amount is accommodated in the higher adsorption potential layers. No lower potential layer can contain adsorbate at equilibrium unless all the higher potentials are full (Noll et al. 1991). Therefore, there is a definite relationship between the adsorbed volume (W) and the adsorption potential (ε). Plots of W vs. ε are termed "characteristic curves" of the adsorbent. The characteristic curve is independent of temperature. Ideally, knowing the characteristic curve for an adsorbent and the affinity coefficient (coefficient which permits the comparison of the adsorption potential of the test adsorbate to a reference adsorbate) of the test VOC enables one to calculate adsorption isotherms for that compound.
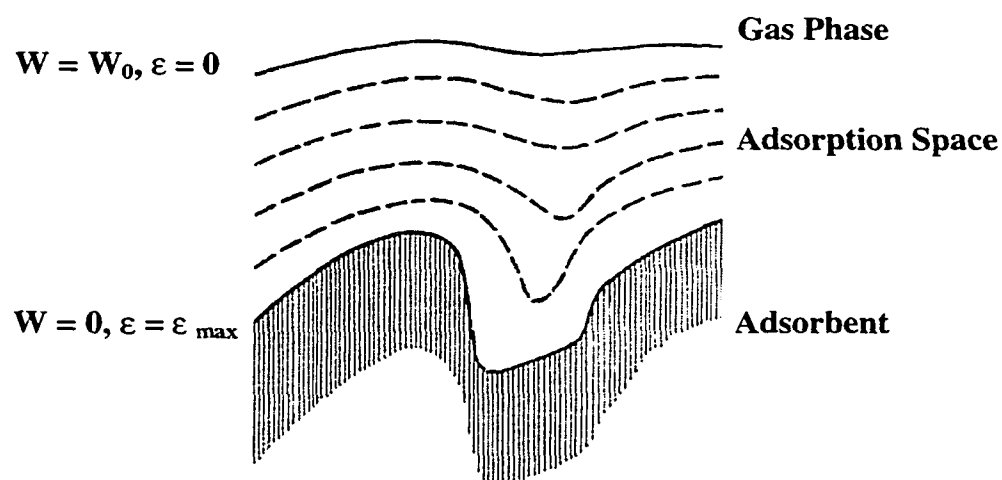
Figure 2.2. Cross Section of the Adsorbed Layer

according to the Potential Theory (*Source:* Young et al. 1962)

19

Dubinin and co-workers defined a general mathematical form of the characteristic curve (Dubinin et al. 1971, Dubinin 1975, Werner et al. 1988), known as the Dubinin-Radushkhevich (DR) equation:

$$\ln W = \ln W_0 - \kappa \left(\frac{\varepsilon}{\beta} \right)^2 \qquad (2.16)$$

The DR equation, however, fails for many gas-solid systems (Doong et al., 1988). During the later stage of the development of the theory of volume filling of micropores, Dubinin et al. found that the initial principles of the potential theory have no physical meaning for adsorption in micropores (Dubinin 1975). They adopted a strict thermodynamic interpretation of the function

$$A = RT \ln \left(\frac{P_s}{P} \right) \qquad (2.17)$$

expressing the differential molar work of adsorption equal, with a negative sign, to the change in free enthalpy. A more general equation (DA equation) proposed by Dubinin and Astakhov may be represented as follows (for activated carbon):

$$q = q_0 \exp \left[-\left(\frac{A}{E} \right)^2 \right] \qquad (2.18)$$

where q is the adsorption at a temperature T and equilibrium pressure p, q_0 is the limiting adsorption value corresponding to the filling of the whole volume of the adsorption space W_0, and E is the characteristic free energy of adsorption.

20

2.3   EFFECTS OF HUMIDITY ON VOC ADSORPTION

Many studies have pointed out that water vapor in the carrier gas could compete with VOCs and may substantially and adversely affect the adsorption of VOCs on activated carbon (Nelson et al. 1976, Moyer 1983, Jonas et al. 1985, Werner 1985). This effect has been demonstrated for different applications of activated carbon, various organic adsorbates, a range of relative adsorbate pressures, and various ambient conditions of adsorption (Werner et al. 1988). In essence, air humidity is a prime factor, which should be considered during the design and operation of carbon adsorption processes.

Numerous factors influence the extent to which humidity affects the vapor phase adsorption process. First, the adsorption of various adsorbates is affected differently, depending largely on their chemical characteristics (Moyer 1983). In general, hydrophobic organic adsorbates are affected by water vapor to a greater extent than hydrophilic adsorbates (Werner 1985, Cal et al. 1996). Second, the concentration of the adsorbate has a significant influence at a given level of relative humidity (Werner et al. 1988). Decreasing the adsorbate concentration generally increases the adverse effect of humidity (Moyer 1983, Werner et al. 1988). Third, the humidity level also influences the magnitude of its effect. Below 50% RH the effect is minimal, however the effect increases with increasing humidity (Nelson et al. 1976, Jonas et al. 1985, Chou et al. 1997). This statement is in line with the observation that the water adsorption isotherm on activated carbon increases sharply at about 50% relative humidity (Okazaki et al. 1978). Lastly, the carbon structure can also influence the magnitude of impact by water vapor. Water molecules are believed to adsorb onto oxidized sites of the carbon adsorbent (Dubinin 1980, Dubinin et al. 1981). The greater the number of oxidized

21

sites on the adsorbent, the greater the interference water molecules can exert on the adsorption of an organic vapor (Werner et al. 1988).

Interference of organic adsorption by water vapor is a special case of multicomponent adsorption. However, multicomponent adsorption theories generally fail in predicting adsorption equilibria of organics and water vapor systems. Therefore, in the literature, special models have been proposed, some of which will be reviewed in the following sections.

2.3.1 Modeling Effects of Humidity on VOC Adsorption

Okazaki et al. (1978) proposed a method to predict the adsorption equilibria of mixtures of solvent and water vapor on activated carbon. The model is based on evaluating the amounts of solvent and water in the capillary condensed phase in the fine pores and in the ordinary adsorbed phase on the surface of the coarse pores, respectively (Okazaki et al. 1978, Doong et al. 1987, and Chou et al. 1997). Figure 2.3 illustrates the proposed adsorption model. According to this model, the organic vapors are adsorbed onto the activated carbon by three different mechanisms: (1) adsorption on the dry surface (those pores in which condensation of water vapor does not take place); (2) dissolution in the condensed water; and (3) adsorption on the wet surface (pores in which condensation occurs). The total capacity of the activated carbon for the VOC is the sum of these components (Okazaki et al. 1978 and Crittenden et al. 1989). The necessary data for this model are: pure component gas-phase adsorption isotherms, liquid-phase isotherms of organics, vapor-liquid equilibria and pore volume, surface area distribution curves for the carbon. A large amount of system data required makes this model cumbersome to use (Doong et al. 1987).

22

VOC Adsorbed on Dry Surface

Porous Adsorbent

VOC Adsorbed on Wet Surface

VOC Dissolved in Condensed Water

Dry Pore

Pore Filled with Water by Capillary Condensation
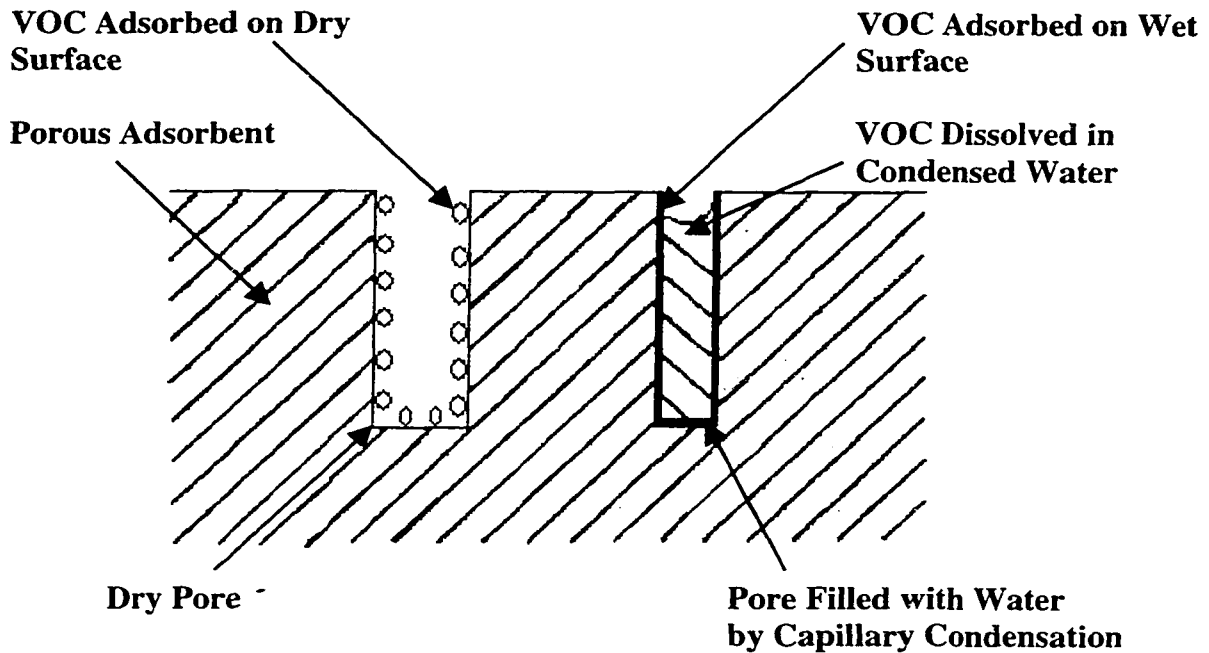
Figure 2.3. Schematic Representation of Okazaki's Model

(Source: Crittenden et al. 1989)

Manes (1984) developed a Polanyi Potential theory based model for estimating the effect of humidity on the adsorption of water-immiscible organic vapors onto activated carbon. It was assumed that adsorbed water reduces the pore space available for adsorption of an organic compound on a one-to-one volume basis. Additionally, Manes assumed that at 100% RH adsorption of any organic vapor is equivalent to its adsorption from a water solution. At 100% RH, the net adsorption potential of the organic vapor is its normal adsorption potential (ε_0^0, associated with its pure-component vapor adsorption in the absence of water vapor) diminished by the adsorption potential of an equal volume of water (ε_w^0), given as:

$$\varepsilon_0 = \varepsilon_0^0 - \varepsilon_w^0 \left(\frac{V_0}{V_w} \right) \tag{2.19}$$

23

Where, V_0 and V_w are molar volumes of the organic and water respectively in their liquid state. Equation 2.19 is applicable to any immiscible organic under the condition that the organic adsorbate volume is less than the volume of adsorbed water. If the organic volume is greater than that of water, no interference results from the presence of water (Werner et al. 1988). Characteristic curves for the pure component adsorption of VOC and water are prerequisite for this model.

For the more generalized case, if the RH is less than 100%, the modified Equation 2.19 becomes:

$$\varepsilon_0 = \varepsilon_0^0 - \varepsilon_w^0 \left(\frac{V_0}{V_w} \right) + \left(\frac{V_0}{V_w} \right) RT\ln \left(\frac{1}{RH} \right) \tag{2.20}$$

The method of solution for the Manes model is somewhat tedious (Cal et al. 1996).

Doong et al. (1987) suggested a model based on Dubinin's theory of volume filling. This model, however, requires solving by a complicated trial-and-error procedure (Tien 1984).

Recently, Chou et al. (1997) proposed a simple Freundlich-like model (Equation 2.21) for adsorption capacities for VOCs in humid air streams.

$$\frac{q_{voc}}{q_{voc, RH=0}} = 1 - k_4 \cdot RH^{1/n} \tag{2.21}$$

Where, q_{voc} is the equilibrium adsorption capacity in an air stream with a relative humidity RH and $q_{voc,RH=0}$ corresponds to that with RH = 0 at the same temperature. The parameters of equation 2.21 can be found by regression analysis.

CHAPTER THREE

MATERIALS AND METHODS

3.1   ADSORBENT

The activated carbon used was type BPL (Calgon Carbon Corporation) in 6×16 mesh form. BPL is a bituminous coal-based virgin granular activated carbon (GAC) activated at a high temperature in a steam atmosphere. Manufacturer's data for the physical properties of the GAC are listed in Table 3.1.

Table 3.1. Physical Properties of BPL 6×16

Property	Value
Approximate Shape	Sphere
Apparent Density (g/mL)	0.47 Min
Moisture, weight %, as packed	2.0 Max
Ash, weight %	8 Max
Iodine No., (mg/g)	1050 Min
Particle Size (weight %)	
> 3.36 mm (US mesh 6)	5.4 Max
< 1.19 mm (US mesh 16)	5.0 Max

Source: Calgon Carbon Corporation

The activated carbon was dried at a temperature of approximately 150°C for 24 hours and subsequently cooled at room temperature in a desiccator before the experiments.

3.2   WATER VAPOR ADSORPTION

3.2.1   Adsorbate

Water vapor (18% < RH < 96%) was selected as the target adsorbate.

25

3.2.2 Experimental Setup

The experimental setup is shown in Fig. 3.1. It consists of three functionally discrete sections: vapor generation, adsorption and detection.

3.2.2.1 Vapor Generation

The compressed air from the laboratory air system was used as carrier gas. A laboratory gas drying unit (Drierite, W. A. Hammond Drierite Co., Ohio) was used to remove oil, humidity and submicron particles. The influent humidity level after the drier was less than 5%. The air was then humidified by diverting a portion of the dry influent air through a water bubbler and then combining it with the dry dilution air. Two flowmeters with built-in controllers (FM044–40C, Cole Parmer) were used to adjust the flow rates (of humid air and dry dilution air respectively) to achieve a particular design humidity level in the influent. Total flow was measured with a rotameter. The rotameter was calibrated using a soap-bubble meter (Universal Pump Calibrator, Inspector's model 302, Environmental Compliance Corp.) and a Dry test meter (175-S Meter, Rockwell Manufacturing Company). Appendix B describes the calibration of the rotameter.

3.2.2.2 Adsorption

The adsorber was a vertically supported glass column, 38.5 mm in inner diameter and 155 mm in height. The lower end of the column had a flat fritted glass support for the carbon bed. The column had a ground glass outer joint at the top. The design of the adsorber was in agreement with the ASTM recommendations (ASTM 1995).

26

27

Pressure Gauge

Thermocouple

Vent

Flowmeters with
Controllers

Online Data
Acquisition

Adsorption Column

Lab Air Drying Unit

Lab Air Supply

Water Bath

Thermo Hygrometer
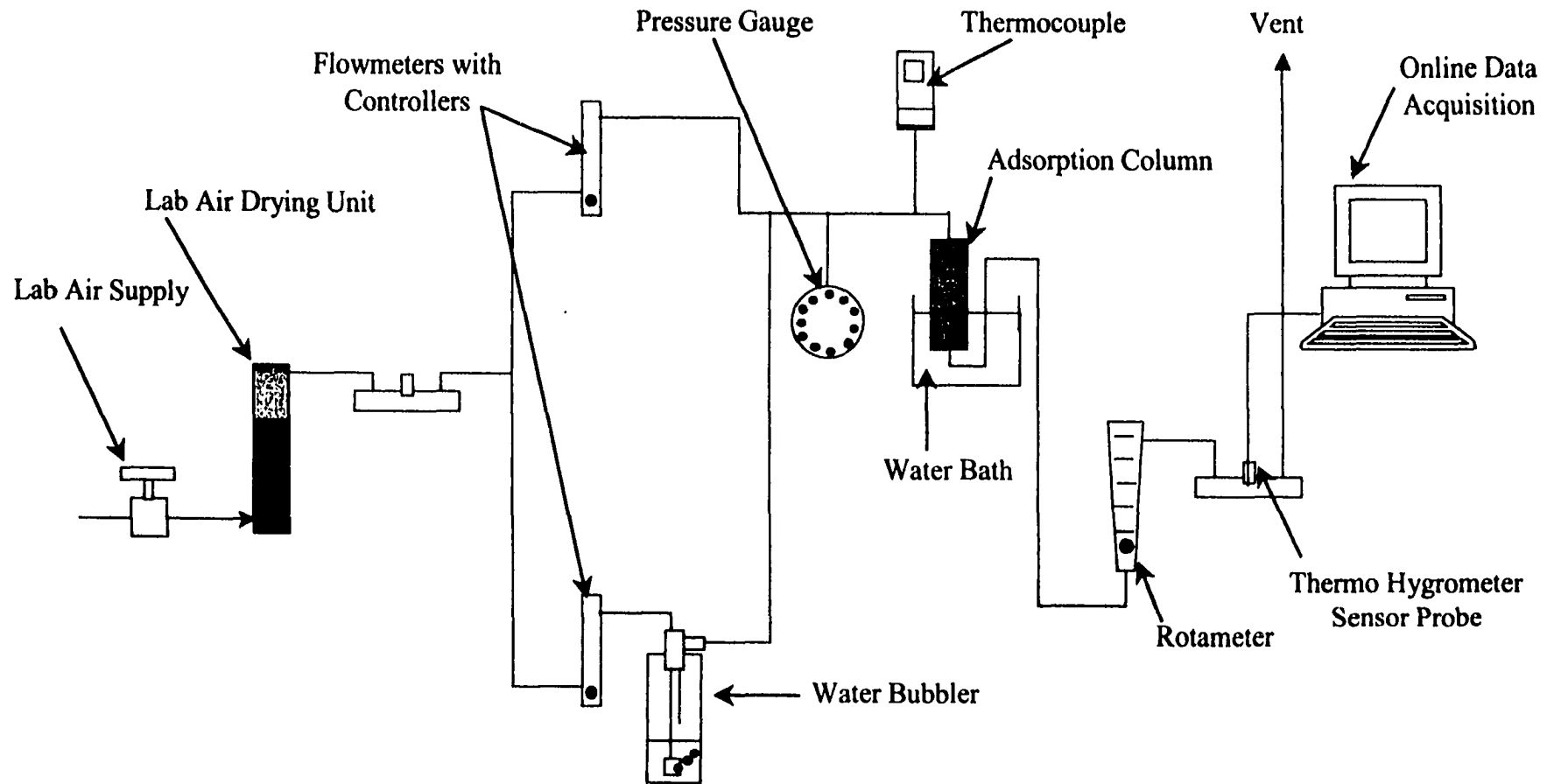Sensor Probe

Rotameter

Water Bubbler

Figure 3.1 Experimental Setup (Water Vapor Adsorption)

Upstream adsorption bed pressure was measured with a pressure gauge (Trerice Pressure Gauge, Trerice Co., Windsor, Ontario).

3.2.2.3 Detection

The relative humidity was measured with a high performance digital thermo-hygrometer (RH411, Omega Engineering Inc., Stamford, Connecticut). Analog signal outputs (10 mV / %RH and 10 mV / $^{\circ}$F) were connected to a computerized data acquisition system (CIO-DAS16/Jr, Computer Boards Corporation, Massachusetts). CIO-DAS16/Jr is a 16 channel 12 bit analog input board capable of data acquisition at 110 KHz. A software package (Snap-Master™, HEM Data Corp., Michigan) was used as the interface. Online data acquisition allowed continuous monitoring of relative humidity and temperature simultaneously.

3.2.3 Procedure

The adsorbent bed weights used in this investigation ranged from 20 to 35 g (dry weight) of activated carbon (corresponding bed height was approximately 35 mm). Parafilm was used to seal the column while weighing to avoid any prehumidification. The column was connected to the system sometimes after the initial start-up period. This was done to avoid the exposure of the carbon bed to the unsteady conditions. The flow direction was downward to avoid fluidization of the bed. The flow rate was maintained at approximately 1 L/min. To maintain an isothermal condition (30°C) the column was placed in a water bath. The temperature of the bed was measured with a T type thermocouple placed between the carbon granules, about 25 mm from the top of the bed. The temperature of the bed varied from 29°C

28

to 31°C. To delineate the kinetics of water vapor adsorption, RH values of the effluent were collected every 40 seconds with the help of the online data acquisition system. To obtain the equilibrium adsorption data, the tests were continued for at least 1 hour past the time when the effluent RH equalled the influent RH. The column was then quickly removed from the system, sealed with parafilm and the adsorbent weight gain was measured using a balance (Mettler AE 163).

3.3   Single Component VOC Adsorption

3.3.1   Adsorbate

Anhydrous m-xylene (99+%, Aldrich) was used as target VOC for adsorption. A concentration range of approximately 50-1000 ppm was considered in this research.

3.3.2   Experimental Setup

The experimental setup is shown in Figure 3.2.

3.3.2.1 Vapor Generation

The vapor generation section was almost identical to the one described in section 3.2.2.1. The only basic difference was that instead of using water in the bubbler, m-xylene was used. The m-xylene vapor was mixed with the dry dilution air to achieve the desired VOC concentration in the influent.

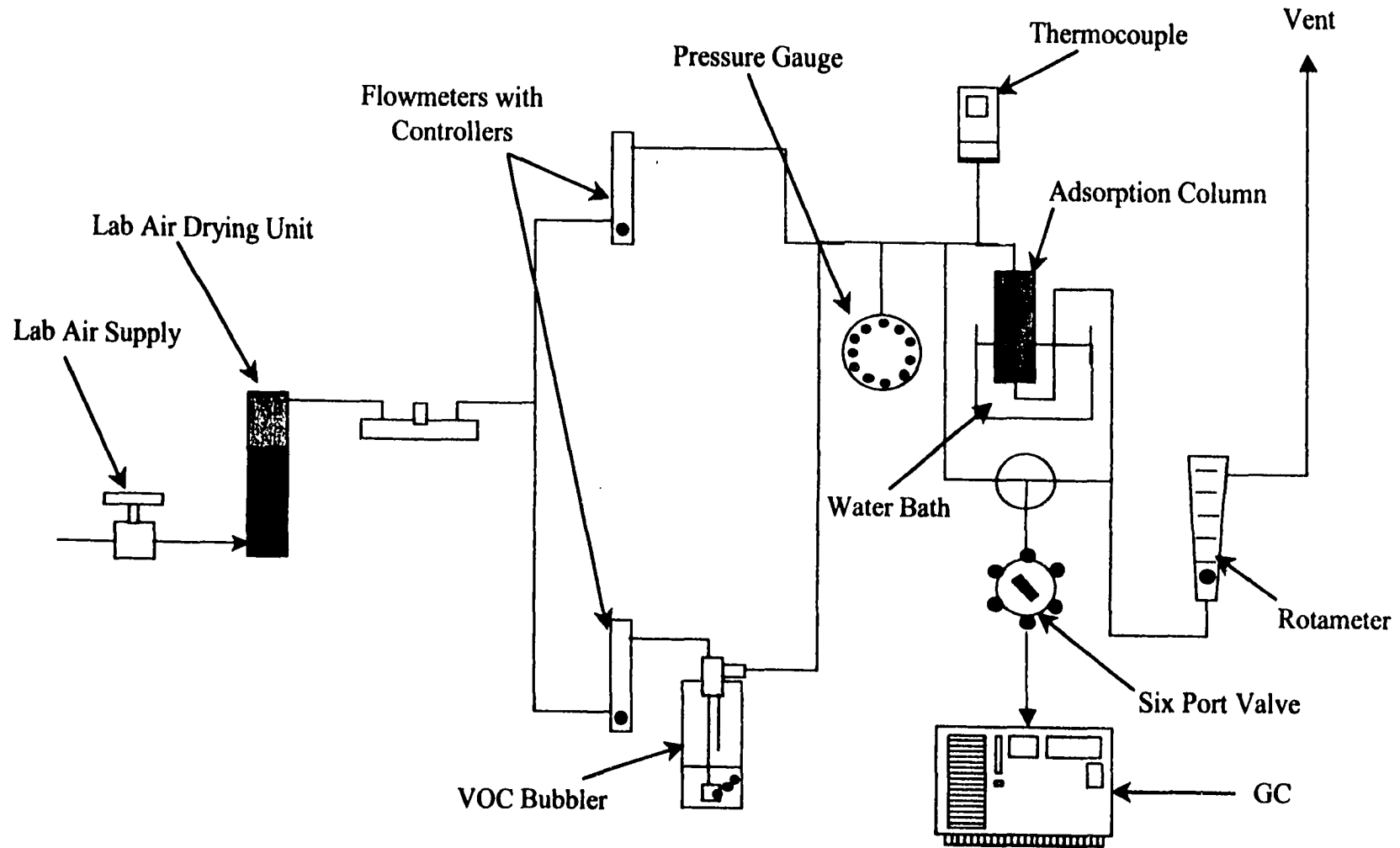#### 3.3.2.2 Adsorption

Same as section 3.2.2.2.

29

Figure 3.2 Experimental Setup (VOC Adsorption)

3.3.2.3 Detection

A gas chromatograph (HP 5890A) equipped with a megabore HP-INNOWax capillary column (30 m × 0.53 mm ID) with a 1.0 μm film thickness (Hewlett-Packard Co.) and a flame ionization detector (FID) was used for the detection of m-xylene. The choice of HP-INNOWax column was based on its high tolerance for moisture content in the samples. To analyze the concentration of the gas streams, a six-port valve system (Valco Co.) with a 250 μL sampling loop was used. Fig. 3.3 shows the detailed description of this valve system. The retention time for m-xylene was 5.87 min using the oven temperature gradient in Table 3.2. The operational parameters of the GC system are given in Table 3.2.

Table 3.2. GC Operational Parameters

Carrier:	Nitrogen, 1 mL/min, Constant Pressure
Oven:	35° C (2.5 min), 10° C/min to 85° C
Injection:	250° C, Split (100:1)
GC System:	HP GC/FID, 300° C

3.3.3 Procedure

The basic procedure was the same as water vapor adsorption. At low adsorbate concentrations the complete saturation takes considerable time. To avoid that, an accelerated testing procedure (ASTM 1995) was adopted for VOC adsorption. It was achieved by increasing the flow rate (to approximately 4 L/min) through the adsorption bed while maintaining the desired adsorbate concentration.

The GC was initially calibrated by 6 standard solutions of m-xylene in liquid tetrahydrofuran (THF; HPLC grade, Fisher Scientific). GC calibration is described in detail
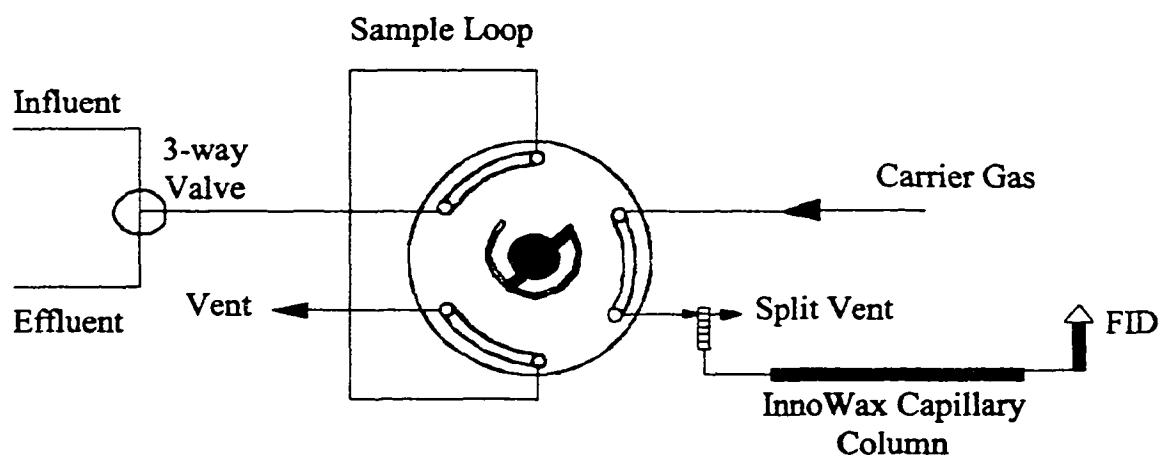
31

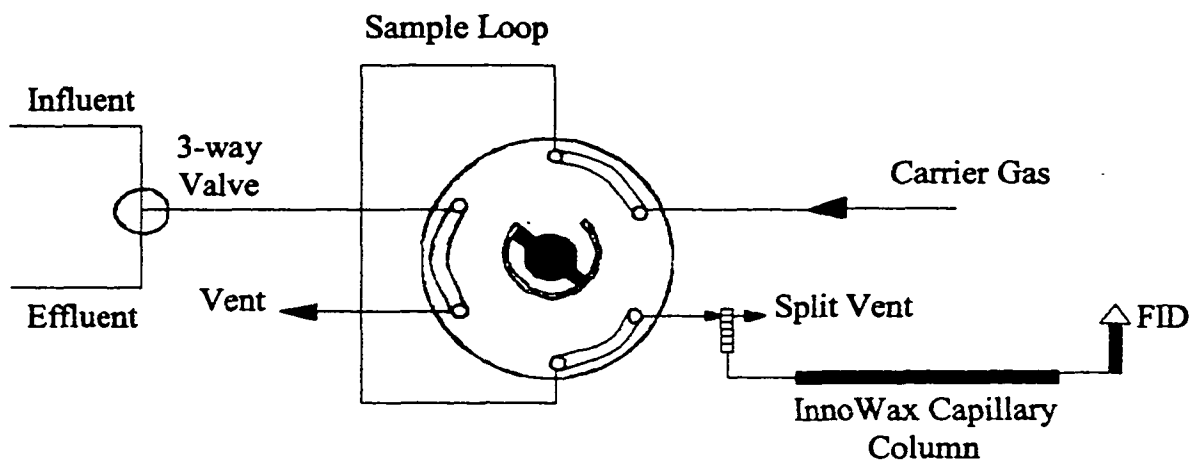**Figure 3.3A   Six-Port Valve System (Running Mode)**

Figure 3.3B   Six-Port Valve System (Sampling Mode)

32

in Appendix C. Two GC liquid standards (143.8 ppm and 545.9 ppm m-xylene in THF) were injected intermittently for quality control also to check the validity of the initial calibration for that particular test day. Figure C.3 (Appendix C) shows the Quality Control Chart for the GC standards used. The adsorber influent and effluent were sampled periodically by diverting the air flow through the sampling loop for five minutes. The VOC concentrations were measured and the GC outputs were integrated with 3392A Integrator (Hewlett-Packard) to evaluate peak areas. The column was considered to be saturated when the effluent concentration became equal to the imposed influent concentration and also the experimental run time was more than that predicted by Wheeler's model (Equation 3.1). Wheeler's model was used as a stopping criterion to avoid pre-saturation stopping due to any measurement error.

$$t_B = \frac{W_e W}{C_0 Q} - \frac{W_e \rho_B}{C_0 K_V} \ln\left(\frac{C_0}{C_x}\right) \tag{3.1}$$

At saturation $C_x = C_0$. Therefore, the second term of Equation 3.1 drops.

As earlier, the column was removed from the system to measure the gain in mass due to VOC adsorption.

3.4   Binary Component Adsorption

3.4.1   Adsorbates

m-xylene (178-1123 ppm) adsorption in the presence of water vapor (54-88 %RH) was investigated.

33

3.4.2 Experimental Setup

Figure 3.4 depicts the experimental setup for the adsorption of the m-xylene/water vapor system. The setup was a combination of the water vapor adsorption experimental setup and the single component adsorption setup. Figures 3.5 and 3.6 show different views of the entire setup. To achieve high humidity levels (>70%) the original setup (Figure 3.4) was modified for some of the runs (run # 9, 10 and 11). Another water bubbler was added in series connection with the VOC bubbler.

3.4.3 Procedure

The same procedure as described in the sections 3.2.3 and 3.3.3 was followed. The stopping criteria were: (1) the inlet humidity level was equal to outlet humidity level; (2) the influent VOC concentration is equal to the effluent concentration. Wheeler's model was not considered as a stopping criteria due to the anticipated change in the adsorption behavior of the VOC in the presence of humidity.
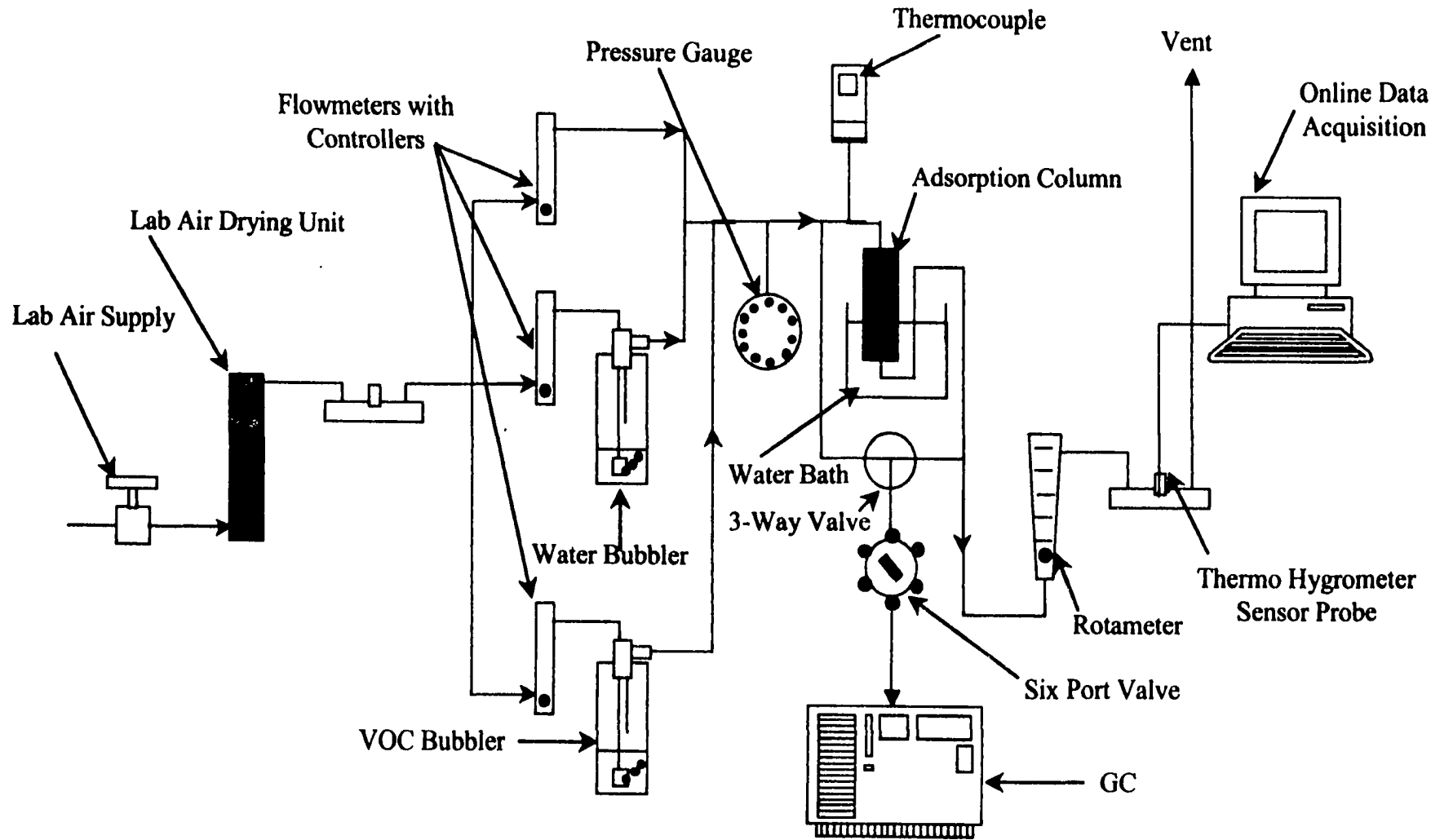
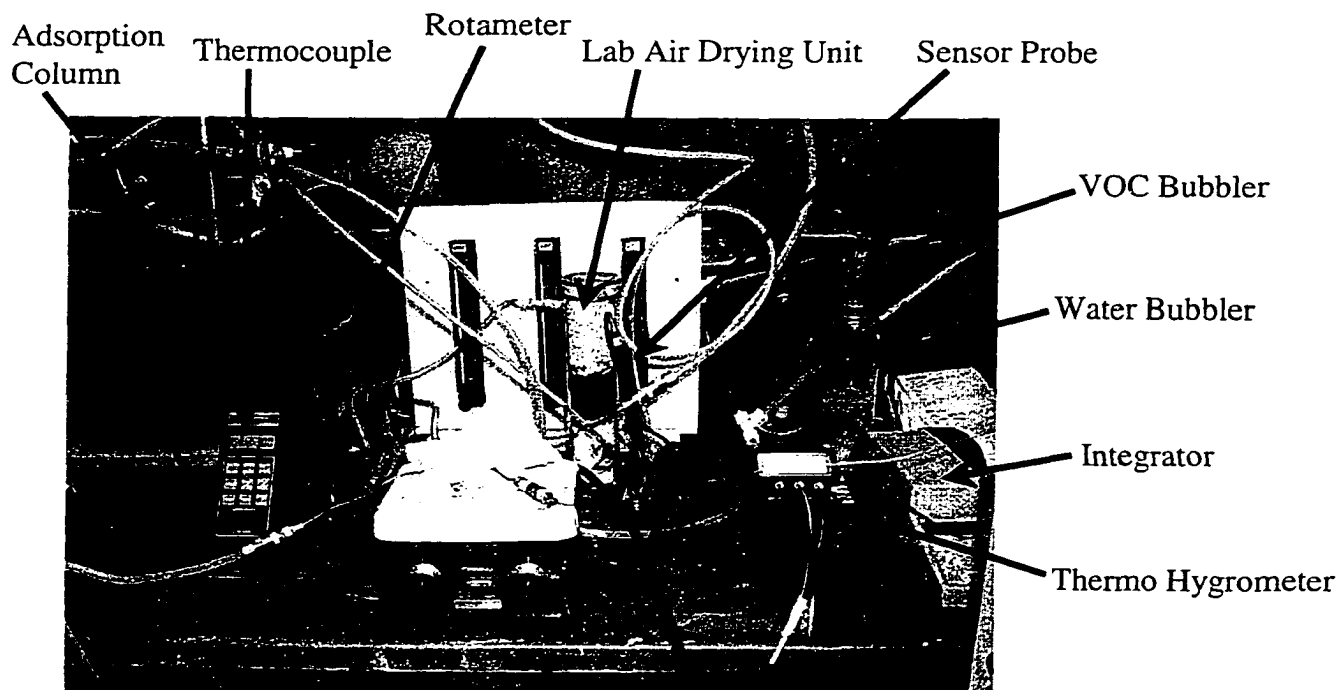**Figure 3.4 Experimental Setup (Mixed Vapor Adsorption)**
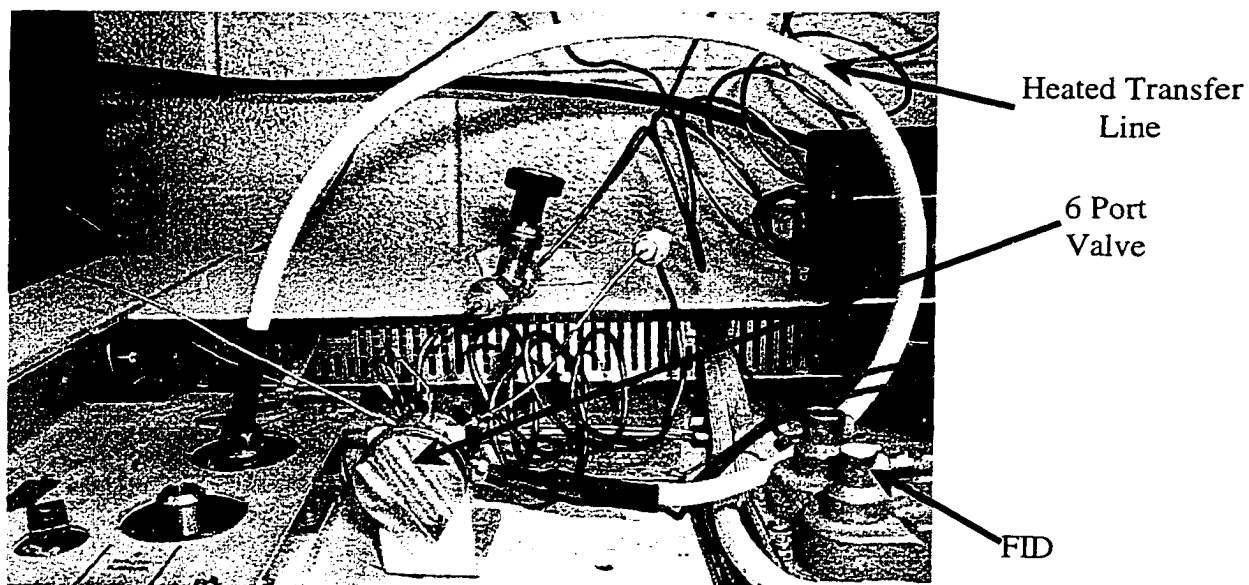
Figure 3.5 Experimental Setup (View 1)

Figure 3.6 Experimental Setup (View 2)

CHAPTER FOUR

RESULTS AND DISCUSSION

4.1 WATER VAPOR ADSORPTION: ADSORPTION EQUILIBRIA

The experimental results for water vapor adsorption equilibria are presented and discussed in this section along with the results and interpretations based on different model predictions.

Equilibrium data are listed in Table 4.1. The adsorbed volume (W or V) is calculated from the adsorption capacity (q) by a simple relation that follows:

$$W = \frac{q}{\rho} \qquad (4.1)$$

where, ρ is the density (at carbon bed temperature of $303°$ K) of compressed adsorbate in the adsorbent pores.

Table 4.1 Water Vapor Adsorption Equilibrium Data

Run #	RH (%)	T^* ($°$ K)	P_s (kPa)	P (kPa)	Initial Mass of Carbon (gm)	Final Mass of Carbon (gm)	q (g/g)	W (or V) (mL/g)
1	18	295	2.643	0.476	34.383	34.448	0.002	0.002
2	32	296	2.808	0.899	26.969	27.102	0.005	0.005
3	42	296	2.808	1.180	27.427	27.701	0.010	0.010
4	52	297	2.983	1.551	23.265	23.614	0.015	0.015
5	65	296	2.808	1.825	29.664	31.226	0.053	0.053
6	68	296	2.808	1.910	20.758	22.261	0.072	0.073
7	89	297	2.983	2.655	28.270	33.293	0.178	0.179
8	96	295	2.643	2.537	22.876	26.798	0.171	0.172

*T is the average ambient temperature during experiment

37

According to Dubinin (1975), the adsorbed substance in micropores in the adsorption force field is similar to a liquid in a strongly compressed state (with a hydrostatic pressure of the order of several hundred atmospheres). As a tentative estimate ρ can be assumed to be equal to the normal liquid density at atmospheric pressure for temperatures below its normal boiling point.

The equilibrium data obtained in this study are somewhat lower than the previous studies (Figure 2.1). The lower capacity of the activated carbon may be due in part to a surface area lower than that of the carbons used in those studies. The properties of carbon change significantly with production lots. Moreover, the adsorption bed temperature in this study was 303° K, which is higher than the temperature (298° K) in those studies. For virtually any physical adsorption process, the capacity of adsorbent decreases as the temperature of the system increases (Young et al. 1962 and Gregg et al. 1967).

A type V isotherm (Brunauer classification system) was observed for the sorption of water vapor on the activated carbon as shown in Figure 4.1.
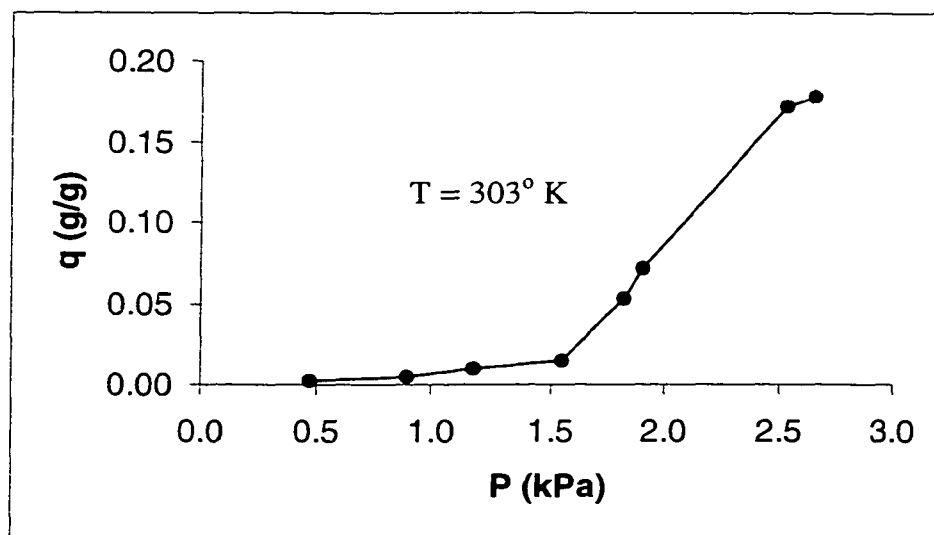

Figure 4.1 Water Vapor Adsorption Isotherm

38

This observation is in accordance with other studies reported in the literature (discussed in section 2.1). From the curve, it is obvious that most of the uptake occurs at RH greater than 55% (the discussions in section 2.1 therefore remains valid).

4.2   MODELING WATER VAPOR ADSORPTION EQUILIBRIA

The equilibrium data were correlated with DS-1, DS-2, DS-3, DS-4 and QHR models. The parameters of DS-1 were determined graphically from the linear form of the model (Equation 2.3). The Levenberg-Marquardt algorithm was applied for the estimation of the parameters of the other models. This nonlinear regression based algorithm was implemented using DataFit™, a commercially available software package. The best-fit isotherm parameters are presented in Table 4.2.

Table 4.2 Isotherm Parameters

Models	a_0 (g/g)	c	k (g/g)	a_s (or q_o) (g/g)	V_0 (mL/g)	P_{50}/P_0	K	MARE (%)
DS-1	0.0090	1.14	—	—*	—*	—	—	—*
DS-2	0.0052	1.56	1.84	0.204	0.205	—	—	7.74
QHR	—	—	—	0.183	0.184	0.708	14.41	36.34

* a_s, V_0 and MARE were not calculated for DS-1 because it was not valid
for RH > 87.7% (calculated from h > 1/c condition)

The DS-2 and QHR models compare favorably with the experimental data for the entire RH range (Figure 4.2). The DS-1 model, as is well known, is applicable only for the initial part of the of the isotherm upswing. The DS-2 model gives the best correlation over the entire pressure range. The QHR model gave fair predictions, but there appears to be an overestimation during the first part of the isotherm. DS-3 and DS-4 models were also tested for the experimental data correlation (not shown here). However, numerical values of some

39

of the regressed parameters were not theoretically feasible (e.g. negative value of a_0). Furthermore the confidence intervals of some of the parameters were very wide (i.e. the standard errors were large); therefore, these models were eventually not included in this study.
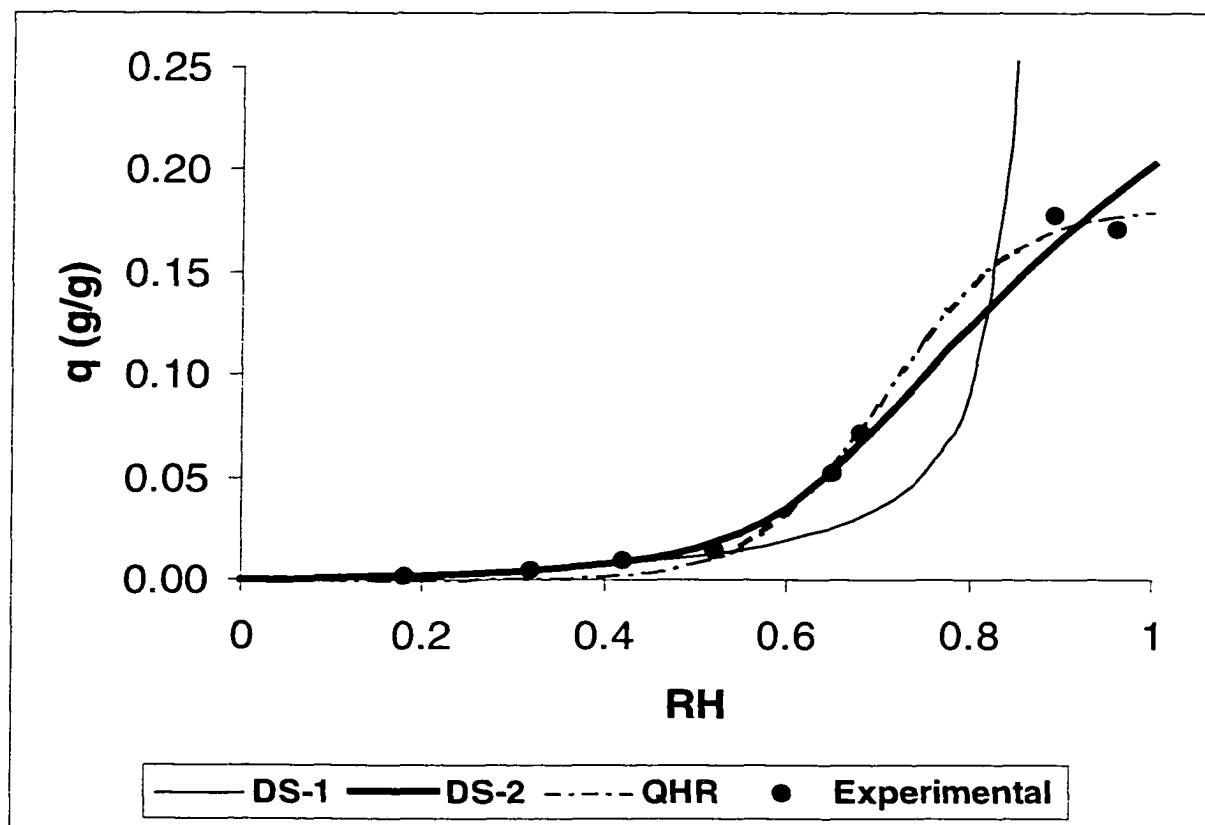

Figure 4.2 Comparisons of Experimental Data to Results from Models

Agreement between the experimental and modeled results is described using the mean absolute relative error (MARE) of q as follows:

$$MARE(\%) = \left(\frac{100}{N}\right)\sum_{i=1}^{N}\left|\frac{q_{i,experimental} - q_{i,modeled}}{q_{i,experimental}}\right| \qquad (4.2)$$

40

where, N is the number of experimental data points, $q_{i,experimental}$ = measured experimental adsorption capacity, $q_{i,modeled}$ = modeled adsorption capacity using the DS or QHR models.

The saturation adsorption, q_0 (or a_s), was obtained by extrapolating the value of q (or a) for RH = 100% using the mathematical models. The limiting pore volume, V_0, is related to the limiting adsorption capacity by Equation 4.1. It is apparent that, although the V_o values depend upon the equation used, their order of magnitude does not change.

4.3   WATER VAPOR ADSORPTION: KINETICS

From the data collected by the online data acquisition system, breakthrough curves were plotted based on the ratio of outlet humidity level to the inlet humidity level versus the adsorption time.
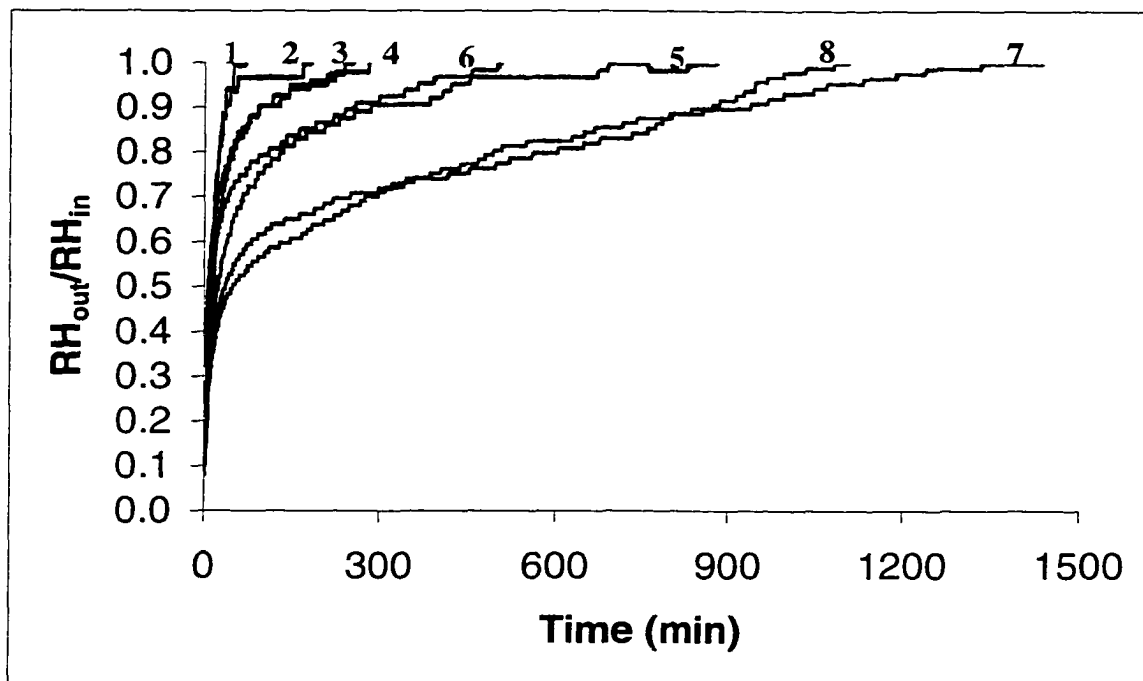

Figure 4.3 Breakthrough Curves

Figure 4.3 illustrates the breakthrough curves for different inlet humidity levels. The numbers 1 to 8 denote different experimental runs with different inlet humidity. Operating conditions for these tests are given in Table 4.3.

Table 4.3 Adsorption Kinetic Experiments

Run #	Inlet RH (%)	Experimental Run Time (min)	Saturation Time (min)	Flow (L/min)
1	18	991	70	1.02
2	32	1183	181	1.04
3	42	1041	253	1.04
4	52	287	281	0.99
5	65	877	877	1.02
6	68	781	505	1.12
7	89	1433	1433	1.08
8	96	1361	1102	0.95

The adsorption capacity at time t (q_t or M_t) was calculated from the breakthrough curve area using a numerical integration scheme (Equation 4.3).

$$q_t = \frac{Q \cdot MW}{w \cdot R} \int_0^t \left[\left(\frac{RH \cdot P_s}{T} \right)_{in} - \left(\frac{RH \cdot P_s}{T} \right)_{out} \right] dt \qquad (4.3)$$

Equilibrium adsorption capacity (q_e or M_e) was calculated considering t = T (stopping time). The values obtained by the integration method were compared with the gravimetric measurement values (Figure 4.4). The difference between the values was approximately 14%. The difference was calculated similar to MARE. Instead of $q_{experimental}$ and $q_{modeled}$, $q_{gravimetric}$ and $q_{integration}$ were used respectively.
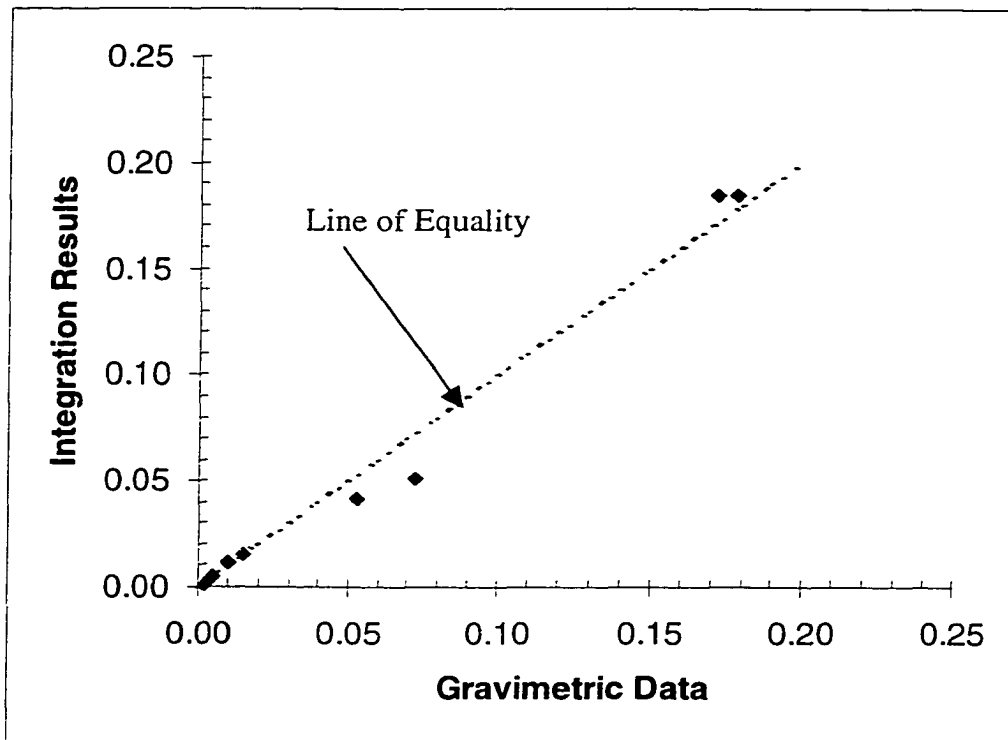
42

Figure 4.4 Comparisons of Gravimetric and Integration Results Data

Typical graphs of $\ln(1 - M_t/M_e)$ versus time are shown in Figures 4.5 through 4.12. Table 4.4 shows the adsorption rate constants. The rate constants were calculated from the gradient of the $\ln(1 - M_t/M_e)$ versus time graph. It is apparent that the rate constant decreases with increasing humidity level. Foley et al. (1997) showed at least three regions of linearity in their kinetic graphs. However, they were unable to show any correlation between the adsorption rate constant and humidity. In this study, instead of dissecting the kinetic curves according to the slopes, overall slopes have been calculated.

The findings of this study can be verified indirectly from the work of Lin et al. (1996). The rate constant k is proportional to the diffusion coefficient. Diffusivity is a strong inverse function of concentration (Foley et al. 1997). Lin et al. reported effective diffusion coefficient values in the range of 3.7×10^{-10} to $2.6 \times 10^{-11} \text{m}^2/\text{s}$ for RH 20 % to 86%.

43
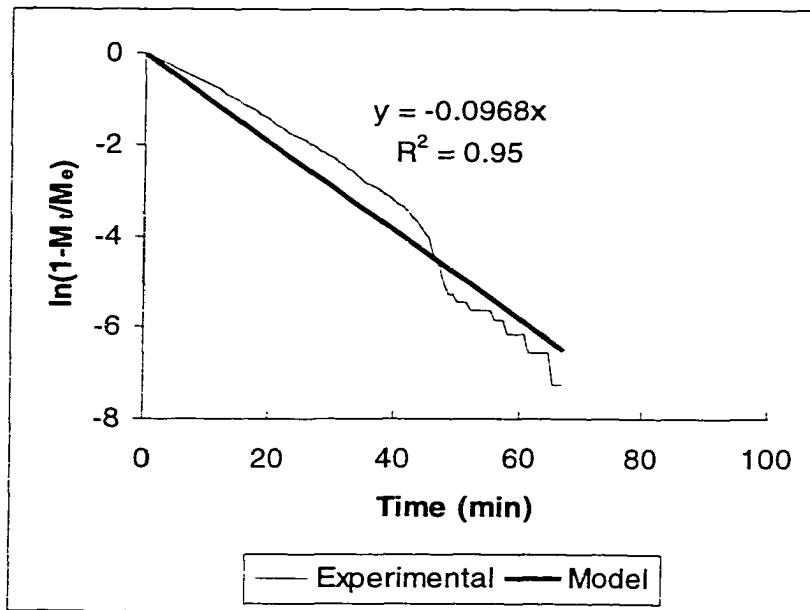
Figure 4.5 Kinetic Graph (RH = 18%)

$$y = -0.0968x$$
$$R^2 = 0.95$$

Figure 4.6 Kinetic Graph (RH = 32%)
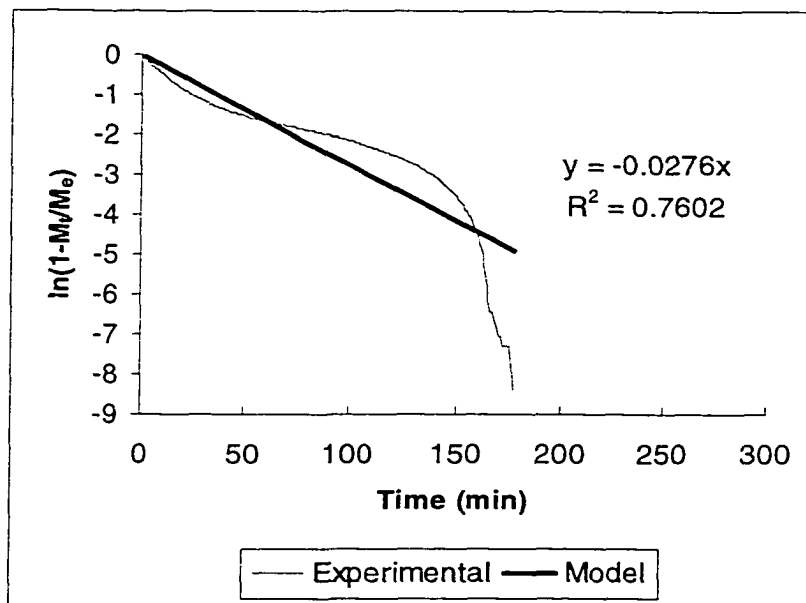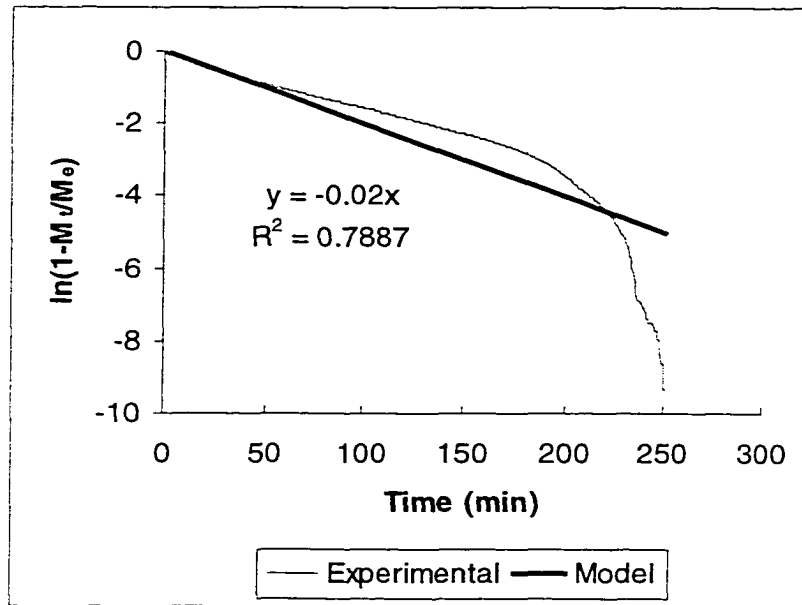
$$y = -0.0276x$$
$$R^2 = 0.7602$$

44

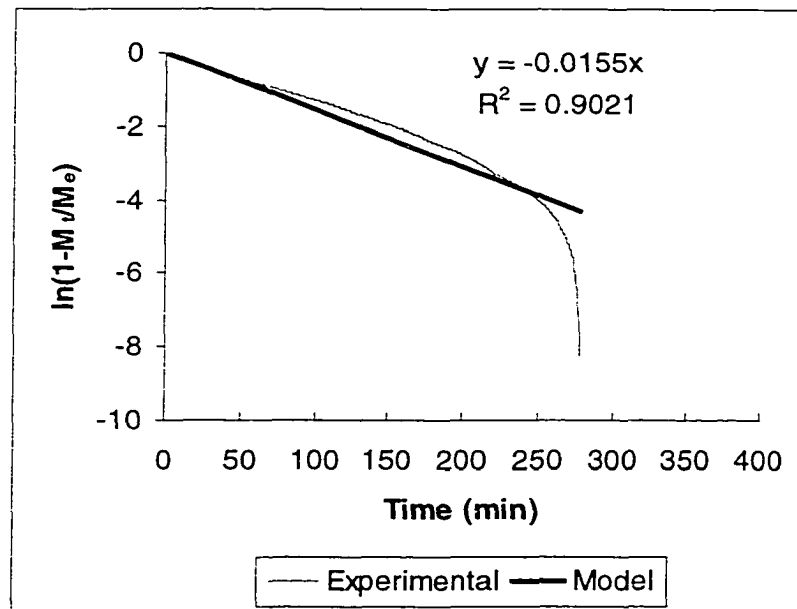**Figure 4.7 Kinetic Graph (RH = 42%)**

Figure 4.8 Kinetic Graph (RH = 52%)

45
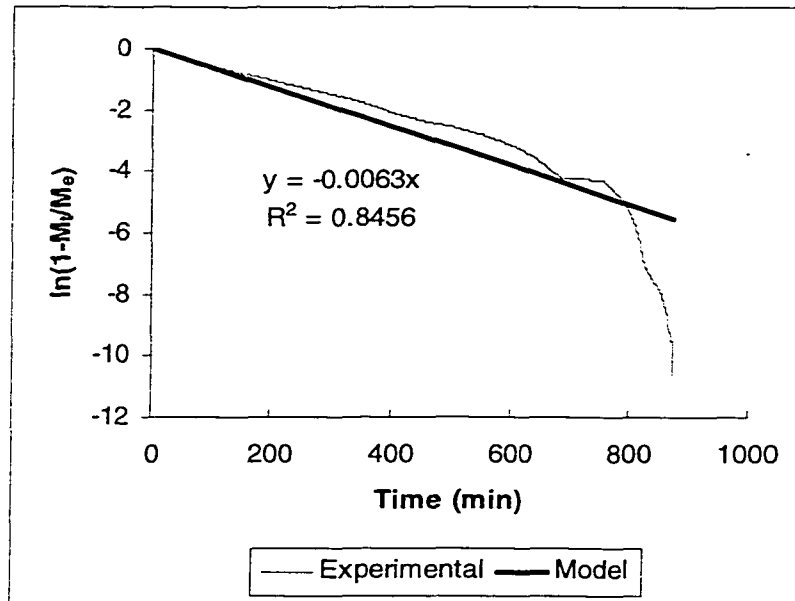
Figure 4.9 Kinetic Graph (RH = 65%)
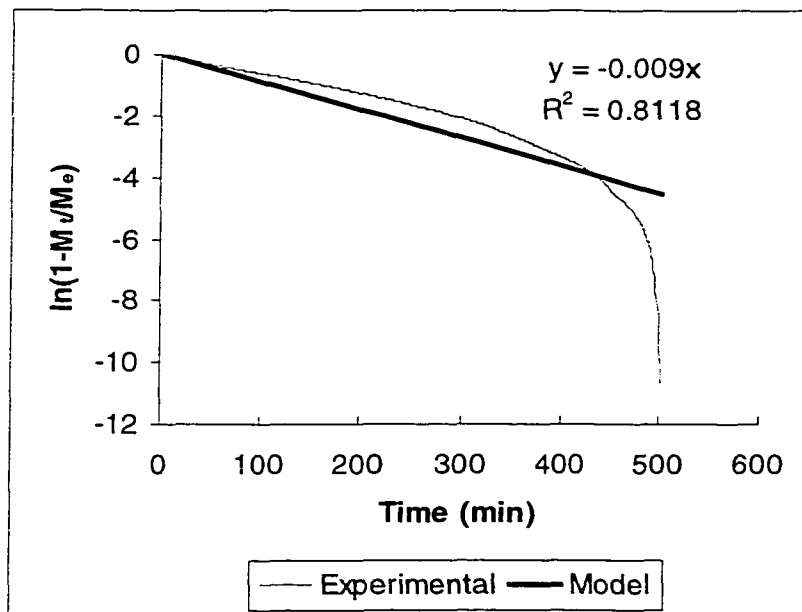
Figure 4.10 Kinetic Graph (RH = 68%)

46
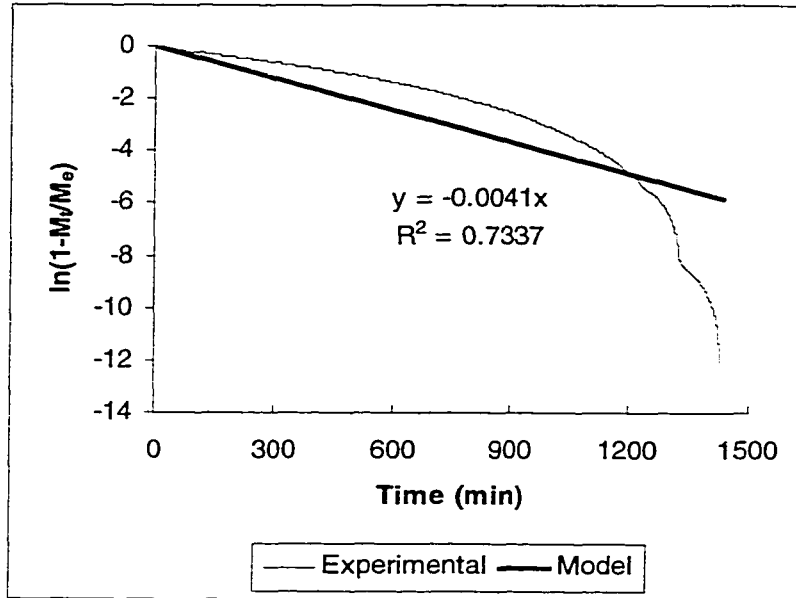
Figure 4.11 Kinetic Graph (RH = 89%)
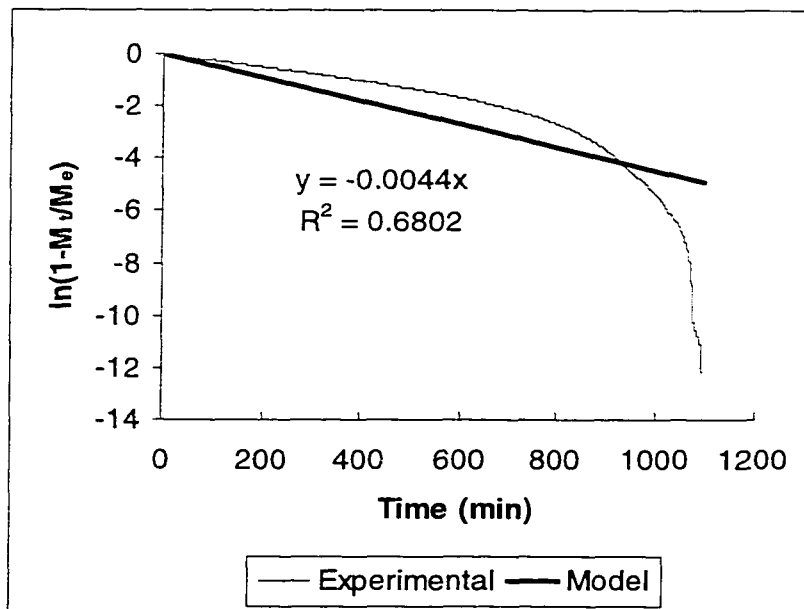
Figure 4.12 Kinetic Graph (RH = 96%)

47

The values of diffusion coefficients decrease with increasing inlet RH. This result indirectly verifies our results.

Table 4.4 Adsorption Rate Constants

RH (%)	k (min^{-1})	b (min^{-1}.g$^{0.5}$/g$^{0.5}$)
18	0.0968	0.0043
32	0.0276	0.0020
42	0.0200	0.0020
52	0.0155	0.0019
65	0.0063	0.0015
68	0.0090	0.0024
89	0.0041	0.0017
96	0.0044	0.0018

The Equations 2.12 and 2.13 are identical in form. The kinetic constant b (Equation 2.12) can be calculated from the rate constant k (Equation 2.13). Column (3) of Table 4.4 shows the values of b for different RH values. It is obvious that the value of b is approximately constant (= 0.002). Lodewyckx et al. (1997) also obtained an approximate value of 0.002 for all the carbon samples. The only exception was dry carbon put into contact with a humidity of 20% (value of b = 0.005). In our case surprisingly the only exception was at 18% RH (b = 0.0043). This anomaly is not clearly understood. Lodewyckx et al. (1997) attributed exceptions in their results to a different water adsorption mechanism (not explained in detail).

4.4 VOC ADSORPTION

Physical properties of m-xylene are listed in Table 4.5. Equilibrium data for m-xylene at 30° C are shown in Table 4.6 along with the predicted and experimental breakthrough times. As mentioned in section 3.3.3, the adsorption column was considered to be saturated when the effluent concentration became equal to the influent concentration (GC analysis) and also when the experimental run time was more than the theoretical run time (calculated by Wheeler's model). In the cases of run 1 and 2, the second condition was not satisfied (intentionally) because, in those two cases several repetitive saturation values were observed by in the effluent gas chromatograph analysis. The Wheeler equation is the simplest kinetic equation but it has several limitations (Werner et al. 1988) and its accuracy is unacceptable for volatile compounds (Nelson et al. 1976). It might be possible that the Wheeler equation overpredicts breakthrough times for low adsorbate concentrations.

Table 4.5 Physical Properties of m-xylene at 303° K

MW	ρ_T (g/mL)	P_{ST} (kPa)	Molar Volume (mL/gmol)	Boiling Point (°K)
106.17	0.856_{303}	1.46_{303}	123.45	412.3

Table 4.6 Adsorption Experiment Data of m-xylene

Run #	C (ppm)	q_e (g/g)	W (mL/g)	Flow (L/min)	Theoretical Run Time (min)	Experimental Run Time (min)
1	52	0.336	0.393	3.66	8879	5160
2	144	0.374	0.437	3.94	2795	2509
3	392	0.403	0.471	3.82	1366	1961
4	413	0.408	0.477	3.63	1365	1320
5	440	0.409	0.478	3.82	1071	1188
6	1030	0.456	0.533	3.31	641	1413

The experimental adsorption equilibrium data were correlated with the Freundlich (Equation 2.14) and Dubinin-Astakhov models (Equation 2.18). The parameters of the

49

models (Table 4.7) were obtained by nonlinear regression analyses (Levenberg-Marquardt algorithm).

Table 4.7 Comparison of Models for VOC Adsorption Equilibrium

Freundlich Model				DA Model				
K_F	f	MARE (%)	R^2	q_0 (g/g)	V_0 (mL/g)	E (cal/mole)	MARE (%)	R^2
0.332	0.099	0.998	0.986	0.479	0.560	5553.56	1.642	0.953

Both the models correlated the experimental data with a MARE of approximately 1%.

Figure 4.13 shows the Freundlich model fit.
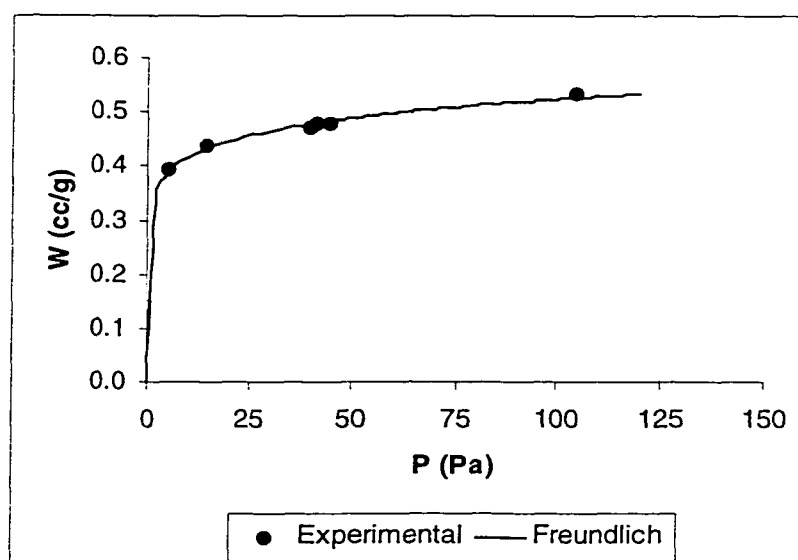
Figure 4.13 VOC Adsorption Isotherm

VOC adsorption isotherm (Figure 4.13) differs qualitatively in shape from the water vapor isotherm (Figure 4.1). The isotherms show pictorially that as a result of m-xylene and water vapor adsorption the adsorbates fill the volume of the micropores of the active carbons. But the nature of filling is quite different. In the case of m-xylene the main micropore volume is filled in the range of small relative pressures. The filling of the main volume of the

50

carbon micropores with water occurs at high relative pressures. Dubinin (1980) pointed out this peculiarity for benzene and water vapor adsorption on the granular activated carbon AG2.

The characteristic curve (section 2.2.1) for the BPL carbon of this study is shown in Figure 4.14. Ideally, this curve can be used to predict the adsorption capacity of this carbon for any adsorbate at any temperature, provided the value of the affinity coefficient is available (Golovoy et al. 1981).
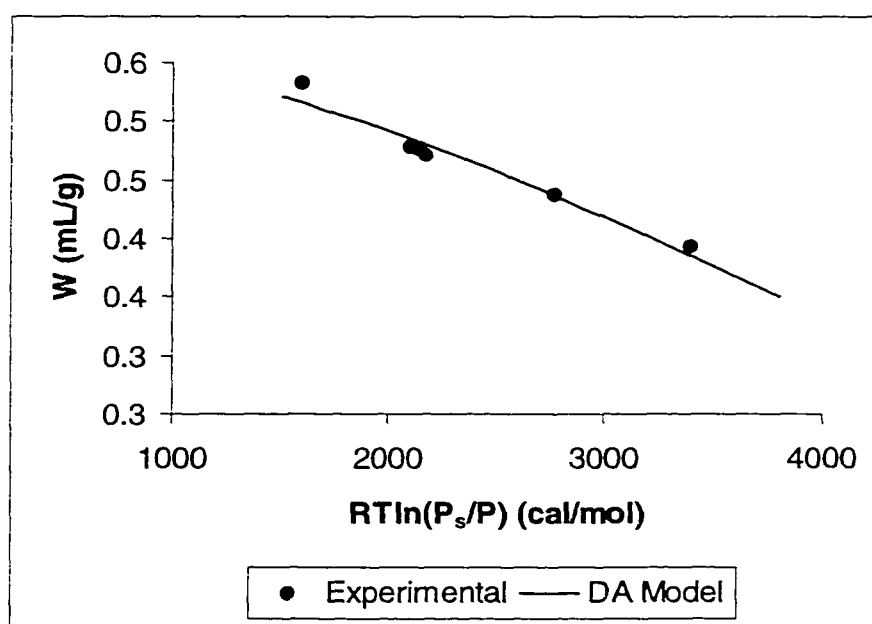
Figure 4.14 Characteristic Curve for VOC Adsorption

As can be seen from the Table 4.7, V_0 has a value of 0.56 mL/g, representing the pore volume of the carbon. But, the pore volume calculated from the water vapor capacity (Table 4.2) is 0.2, much less than that obtained by VOC adsorption. Ideally, the limiting volume adsorbed by a porous adsorbent should be constant and independent of the adsorbate. In other words, a porous adsorbent has a fixed pore volume (Carrott et al. 1995). In some cases, the

51

apparent micropore volume decreases as the molecular size increases. In other cases, there is apparently no relationship between the micropore volume and molecular size. For example, water, which is normally considered to be a small molecule, has a tendency to give a somewhat low value for the micropore volume (Carrott et al. 1995). This observation has been reported in the literature with values of the pore volume calculated from water vapor adsorption at RH ~ 90% to total pore volume from nitrogen adsorption at 77 K in the range of 0.22 – 0.90 (Foley et al. 1997). In this study we observed a ratio of 0.36 (= $V_{0,water}/V_{0,VOC}$). This phenomenon lacks suitable explanations. Carrott et al. (1995) have proposed that water vapor adsorption only occurs in pores of slit-width $\geq$ 0.37 nm, due to the inability of adsorbed water to form a stable hydrogen-bonded structure in narrower pores. Further investigation in this direction was beyond the scope of this study.

4.5   EFFECTS OF HUMIDITY ON VOC ADSORPTION

The effect of moisture on VOC adsorption allows three possibilities: adsorption will be degraded, it will be unaffected or it will be enhanced (Jonas 1985). This study aims to delineate the nature of this interference (positive or negative) by humidity on m-xylene adsorption.

The experimental data of adsorption equilibrium for m-xylene and water vapor mixture are listed in Table 4.8. The pure component values ($q_{0,water}$ and $q_{0,VOC}$) are also listed in Table 4.8. The values of $q_{0,water}$ and $q_{0,VOC}$ were predicted by the DS-2 model and Freundlich model respectively. The binary component (VOC/humidity) resulted in the total adsorption capacity ($q_{water} + q_{VOC}$) of the activated carbon. To find the contribution of water (q_{water}) in the total capacity, area integration (using Trapezoidal rule) of the breakthrough

52

curves of water vapor adsorption was applied. The amount of VOC adsorbed (q_{VOC}) was determined by the material balance of the total experimental adsorption capacity data (gravimetric data) and the water vapor adsorption data (integration method).

Table 4.8 Adsorption Equilibrium Data for Mixed Vapor

Run #	C (ppm)	RH (%)	$q_{0,water}$ (g/g)	$q_{0,VOC}$ (g/g)	q_{water} (g/g)	q_{VOC} (g/g)
1	178	88	0.159	0.378	0.085	0.301
2	202	62	0.042	0.383	0.058	0.323
3	221	54	0.021	0.387	0.029	0.338
4	272	54	0.021	0.395	0.008	0.395
5	795	88	0.159	0.439	0.000	0.427
6	1120	66	0.058	0.454	0.000	0.438

In order to draw conclusions, the results presented in Table 4.8 are transformed into a matrix table (Table 4.9) and a surface plot (Figure 4.15). For the sake of convenience, the entire RH region (18% < RH <96%) was divided into three humidity levels: low (L: < 60%), medium (M: 60% < RH < 80%) and high (H: > 80%). Similarly, the VOC concentration range (50 ppm < C < 1200 ppm) was divided into two levels: low (L: < 250 ppm) and high (H: > 250 ppm). These demarcation lines are true only for this work and the definitions of low, medium or high levels should not be considered as generalized ones.

Table 4.9 Matrix Table

		VOC Levels	
		L	H
RH	L	0.873	1.000
Values	M	0.843	0.965
	H	0.796	0.973

The values in the matrix (Table 4.9) denote retained adsorption capacity ($q_{voc}/q_{0,voc}$). These retained adsorption capacity values are in accord with the literature values (0.09 to 0.87 for a test humidity range of 80% to 90% for 13 different adsorbates) compiled by Werner (1985).
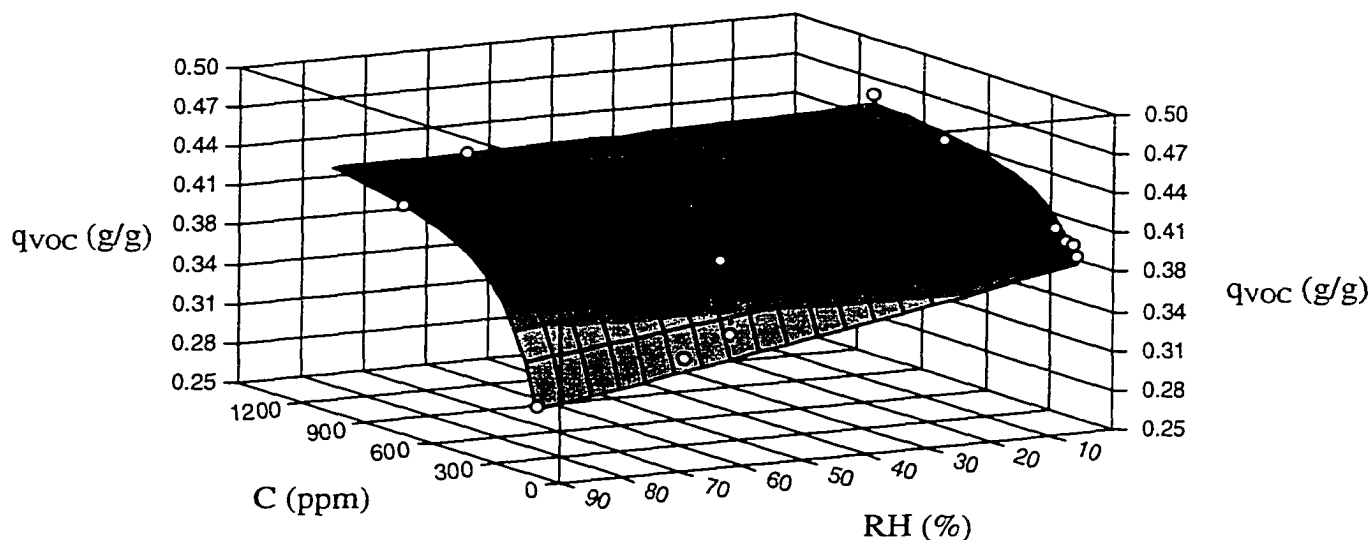
Figure 4.15 Surface Plot of Mixed Vapor Adsorption

The matrix table and the Figure 4.15 indicates that in general, each increase of humidity level further decrease the carbon's adsorption capacity for VOC. The lower the VOC concentration, the more profound the effect of water vapor is on the VOC adsorption capacity of carbon. In the case of high VOC concentrations, the effects of humidity at all levels are almost nil. This finding is consistent with a Russian study referred by Jonas et al. (1985) which found that at high benzene concentration the presence of moisture in the benzene stream had virtually no effect on the sorptive capacity of the carbon for benzene

54

vapor. This was attributed to the very slow adsorption of water vapor by activated carbon and the displacement of initially adsorbed water vapor by benzene.

Applying a "multiplier factor" determined at one adsorbate concentration to account for a given humidity at other adsorbate concentration is commonplace. Multiplier factor is used as a tool to account for the effect of humidity on the adsorption capacity. But, from the above discussion it is obvious that the concept of multiplier factor is not reliable. Because, low concentrations of adsorbates are affected by a given level of humidity to a greater extent than higher concentrations. Werner et al. (1985) questioned the validity of this multiplier factor and suggested additional research in this direction.

The enhancement of adsorption is rather uncommon. The reason for an increase in the adsorption capacity for water in two of the binary states (column 6, Table 4.8) compared to their corresponding single component state values (column 4, Table 4.8) is unclear.

The experimental data was regressed to Chou et al.'s model (Chou et al. 1997). Although the Manes model is theoretically sound, as mentioned earlier, this model is applicable if and only if the adsorbed organic volume is less than the adsorbed water volume. Otherwise the model assumes no interference from the presence of humidity. As discussed in section 4.4 the adsorbed water volume was only 37% of the adsorbed VOC volume at the saturated state. Even the minimum VOC adsorbed volume (0.39 mL/g) was much higher than the adsorbed water volume at 100% RH (0.2 mL/g). This is why the Manes model was not applied for data prediction.

Figure 4.16 shows the comparisons of the experimental and modeled (Chou et al.'s model) results for the low VOC concentration level. The parameters of the model ($k_4 = 0.0037$ and $n = 1.116$) were obtained by nonlinear regression analysis of the experimental

data points. The good agreement (MARE = 0.4% and r^2 = 0.996) between the modeled and the observed results shows the validity of Chou et al.'s model. The model, although shown to be valid in correlating the retained adsorption capacity and relative humidity, cannot be used to predict the quantitative effect of humidity on the activated carbon adsorption capacity for a specified VOC at an equilibrium temperature (Chou et al. 1997).
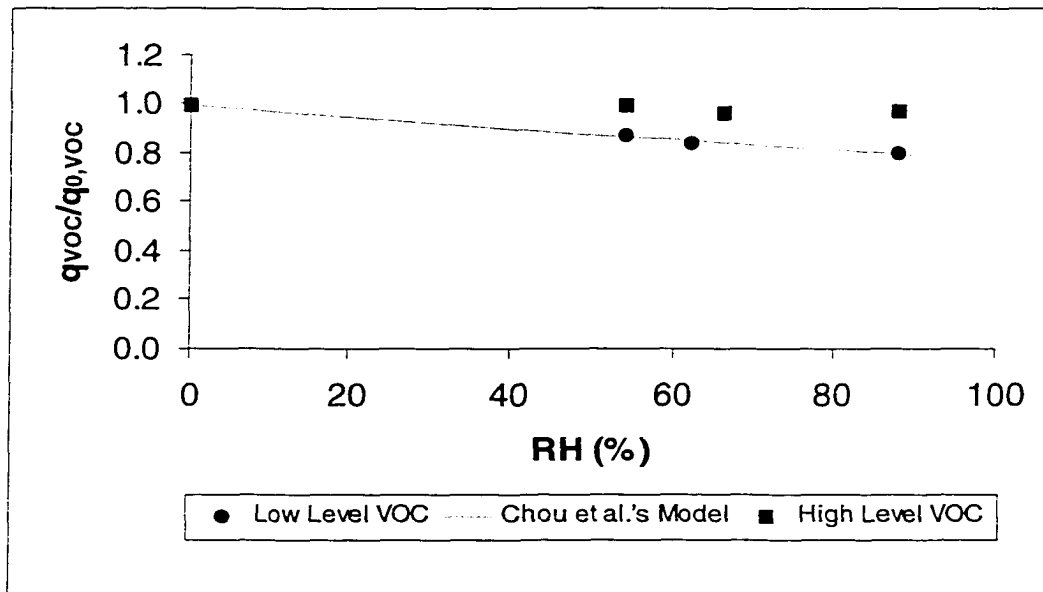
Figure 4.16 Variation of Retained Adsorption Capacity with RH

During run # 5 and 6, "rollover phenomena" was observed (Figure 4.17). The breakthrough curves of water appear with a hump at which the outlet concentration is higher than the inlet concentration. Water is a polar molecule. Its affinity to activated carbon (non-polar surface) is much smaller than that of m-xylene. In addition, the molecular size and molecular weight of water is smaller than m-xylene. So, water has higher diffusion velocity. Thus, water eluted much earlier than m-xylene. The elution order is also determined by the adsorbability of the components. The more strongly adsorbed component (m-xylene) can displace the less adsorbed component (water) from the adsorption site it has already occupied

56

and thus force it to desorb. The replacement of the weakly adsorbed component (water) results in an increase of its concentration in the gas phase since this increased concentration at any time is equal to its inlet concentration plus its desorbed concentration (Gong et al. 1993).
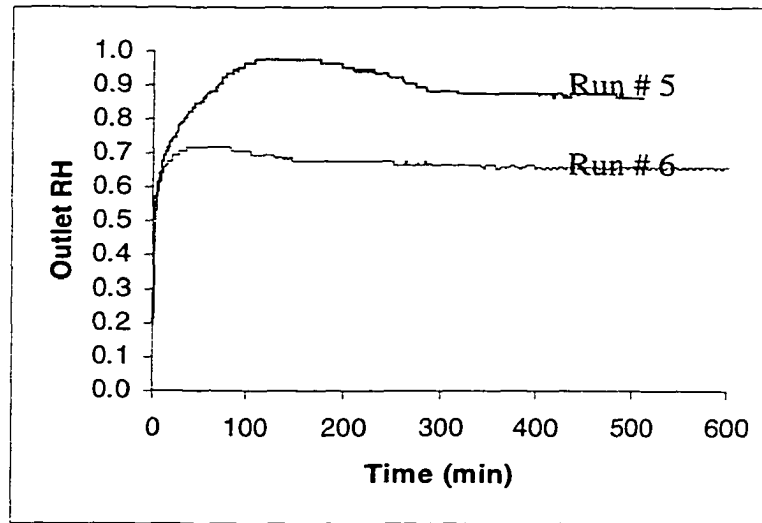
Figure 4.17 Breakthrough Curves for Water Adsorption
(Binary Component Adsorption)

This rollover phenomenon posed difficulties in the integration by Trapezoidal rule. For these two runs (run # 5 and 6), the breakthrough curves were fitted with polynomial curves (5th degree and 10th degree respectively) prior to integration. The areas of adsorption and desorption were calculated separately. The net integrated areas gave small negative values of water adsorption (0.02 and 0.09), which is theoretically not feasible. In this study these negative values were assumed to be zero for further calculations. The following figure illustrates the basics of the rollover phenomena. A_a denotes the adsorbed area and A_d the desorbed area.

57
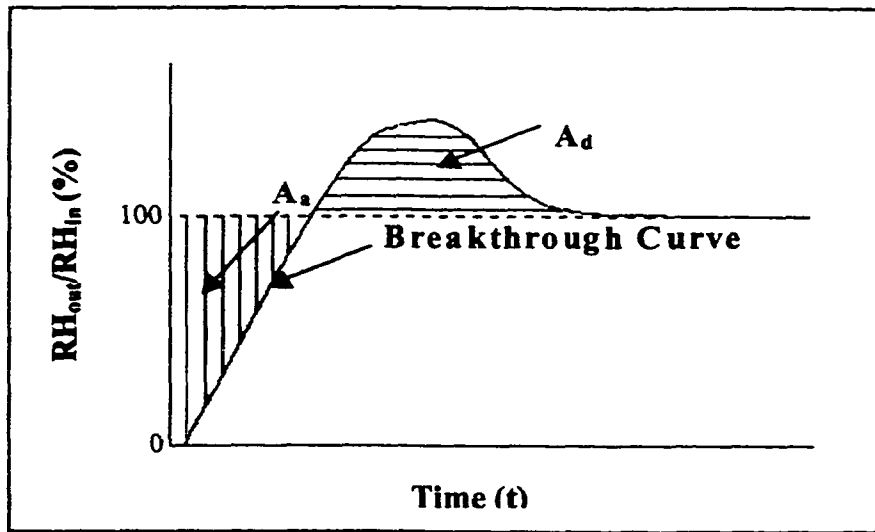
Figure 4.18 Illustration of the Rollover Phenomena

58

CHAPTER FIVE

CONCLUSIONS AND RECOMMENDATIONS

5.1   Conclusions

Summarizing all of the experimental and analysis results, the following useful conclusions are obtained:

1. Water vapor adsorption follows a type V adsorption isotherm and most of the uptake occurs at relative humidities greater than 55%.

2. The kinetics of water vapor adsorption can be satisfactorily represented by the generalized model of Lodewyckx et al. (Equation 2.12) with a kinetic constant equal to 0.002.

3. The adsorption of m-xylene follows type I isotherm and most of the filling occurs at low partial pressures.

4. Pore volume calculated from water vapor adsorption is much less than the VOC adsorption. So, water vapor adsorption should not be used as an inexpensive method for pore volume estimation. This is in contradiction with the statement of Qi et al. (1998).

5. Increase in humidity level leads to decreased VOC capacity. But, low concentrations of adsorbate are affected by a given level of humidity to a greater extent than higher concentrations.

59

5.2   Recommendations

This study provides some fundamental information on the adsorption of m-xylene and water vapor on activated carbon. From the theoretical and experimental findings of this research, several future research directions are recommended as follows:

1. In this study dry activated carbon was used as adsorbent. The effect of preconditioning was not observed. The test humidity has different influences on the adsorption capacity than the preconditioning humidity. The magnitude of this influence remains unresolved. Further research might resolve this issue.

2. The Manes model is valid for water immiscible compounds. A similar model should be developed for water miscible compounds. Moreover, Manes model is valid if the volume of water adsorbed is more than VOC volume adsorbed. The model should be modified to extend its applicability.

3. The pore size and pore volume distribution of the carbon should be determined to understand the pore volume discrepancy as reported in this work (section 4.4). This distribution graph will also aid in the application of Okazaki et al's model (Noll et al. 1992).

4. The kinetics of VOC adsorption in the pure state and in the presence of humidity should be studied.

5. The characteristic curve for BPL activated carbon (section 4.14) should be verified with other adsorbates (with different affinity coefficients).

6. Temperature variation in the adsorption bed was not studied here. This could be a potential area of research.

7. Most of the applications of activated carbon involve mixtures of contaminants. However, as the number of components increases, the required experimental effort becomes more tedious and time consuming. Yet, multicomponent adsorption with humidity effects would be a fruitful research area.

APPENDIX A

PAINT SOLVENTS

Table A.1. Typical Paint Solvents Used in Automotive Coating Applications

Serial #	Compound	CAS Registry Number
1	Acetone	67-64-1
2	Aliphatic hydrocarbons	8032-32-4
3	Aliphatic naphtha	64742-89-8
4	Amyl alcohol	6032-29-7
5	Butyl alcohol	71-36-3
6	Butyl cellosolve acetate	112-07-2
7	DI water	7732-18-5
8	Diacetone alcohol	123-42-2
9	DIBK	108-83-8
10	Diethylene glycol monobutyl ether	112-34-5
11	DPM glycol ether	34590-94-8
12	EEP glycol ether	763-69-9
13	Ethyl acetate	141-78-6
14	Ethyl alcohol	64-17-5
15	Glycol monobutyl ether	111-76-2
16	Heptane	142-82-5
17	Hexyl cellosolve	112-25-4
18	Isobutanol	78-83-1
19	Isobutyl acetate	110-19-0
20	Isopar E	64741-66-8
21	Isopropanol	67-63-0
22	MEK	78-93-3
23	Methanol	67-56-1
24	MIBK	108-10-1
25	Mineral spirits	64742-47-8
26	n-butyl acetate	123-86-4
27	n-propyl alcohol	71-23-8
28	Odorless mineral spirits	64741-65-7
29	Propasol-B	5131-66-8
30	Propylene glycol monomethyl ether	107-98-2
31	Solvesso 100	64742-95-6
32	Toluene	108-88-3
33	m-xylene	108-38-3

Source: Personal communications with Mr. A. S. Mancina (Daimler-Chrysler)

62

Table A.2. Typical Compositions of Solvents Found in Automotive Paints

	Solventborne	Waterborne	Non-aqueous dispersion -acrylic enamel
DIBK	5-20%		5-30%
Aliphatic Naphtha	5-15%		5-20%
Acetone			5-20%
Water		30-50%	
Butyl carbitol	0-5%		
n-Butyl acetate	25-55%		5-15%
Xylene	5-25%		5-25%
Mineral spirits		1-5%	1-5%
n-Butoxypropanol		5-15%	
Propylene glycol monomethyl ether		0-5%	

Source: Personal communications with Mr. A. S. Mancina (Daimler-Chrysler)

63

APPENDIX B

ROTAMETER CALIBRATION

B.1   ROTAMETERS

The rotameter is the most widely used device for measuring gas flow rates. It is a round glass tube of constantly varying inside diameter, which houses one or more floats, which are free to move vertically. It has permanently engraved reference scales on its outer surface. As the gas flows up the tube, the float is displaced and continues to move upward until the gravitational force on the float equals the upward drag force of the moving gas stream. Any change in the flow rate causes the float to occupy a proportionally different position (Nelson 1971).

B.2   FLOW RANGES

The flow range of the rotameter (Matheson Co.) used, was 0 - 5.85 L/min. The rotameter was calibrated with the help of a primary standard (soap bubble meter) and an intermediate standard (dry test meter). The soap bubble meter (Universal Pump Calibrator, Inspector's model 302, Environmental Compliance Corp.) has a maximum working flow rate of 1.5 L/min. Whereas the dry test meter (175-S Meter, Rockwell Manufacturing Company) measures flows greater than 16 L/min with reasonable accuracy and its accuracy declines below 16 L/min. Figure B.1 shows the plot of air flow vs. percentage error for the dry test meter. Figure B.2 shows the calibration curve for the dry test meter (calibration test was done by Central Meter Shop, Union Gas, Chatham, Ontario). The error was defined as: Error = Measured Value – True Value.
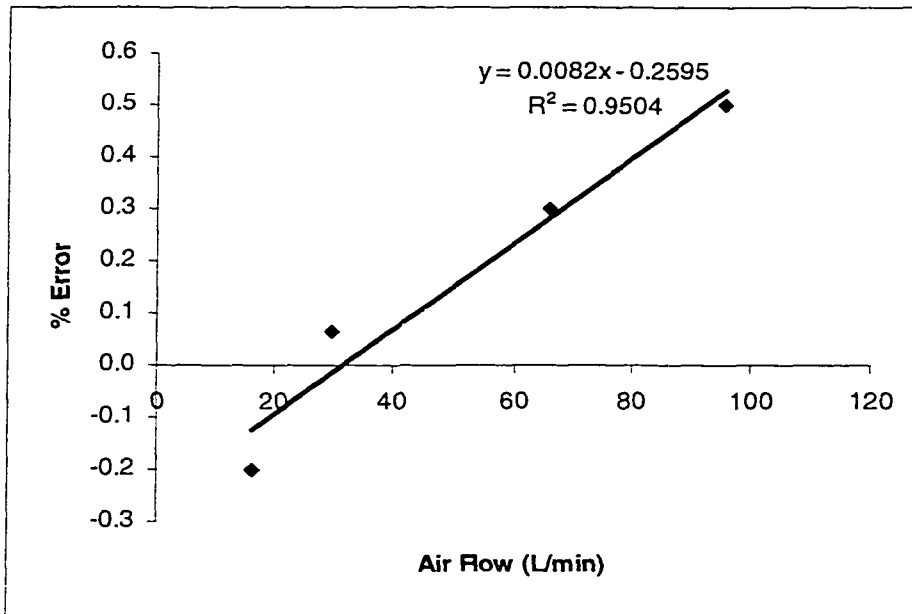
64

Figure B.1. Dry Test Meter Calibration (Air Flow vs. Error Plot)

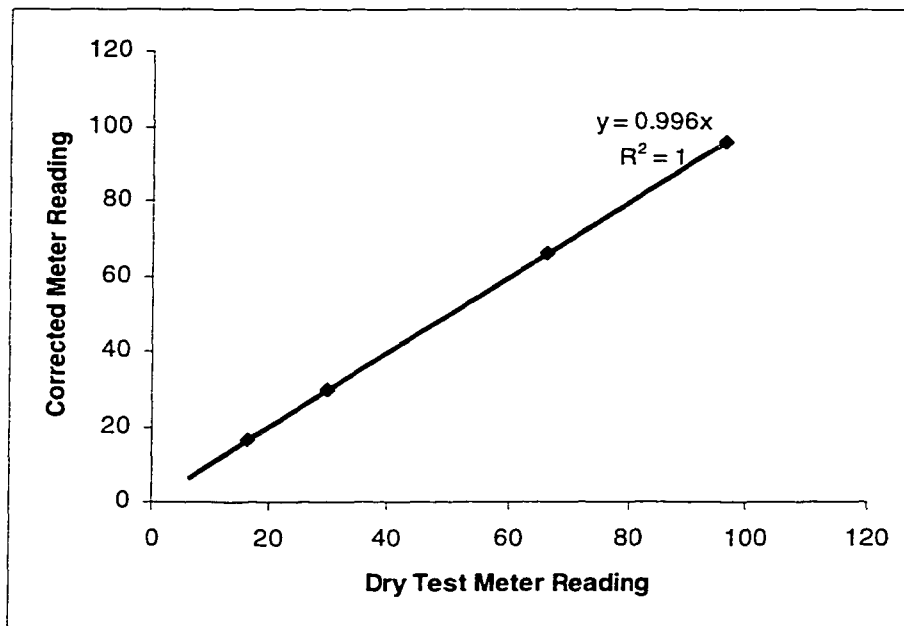(*Source:* Central Meter Shop, Chatham, ON)

Figure B.2. Dry Test Meter Calibration Curve

65

B.3   ROTAMETER CALIBRATION

For the low flow range (less than 1.5 L/min) the rotameter was calibrated using the soap bubble meter. And to calibrate the rotameter in the 1.5 – 5.6 L/min (maximum flow rate used in this investigation was 3.5 L/min) range, the means of the extrapolated soap bubble meter readings and dry test meter readings were considered. Figure B.3 shows the setup for calibrating the rotameter against the soap bubble meter. In the case of calibration using the dry test meter, the soap bubble meter was replaced by the dry test meter (not shown here). Otherwise the set up was identical to Figure B.3.

Soap Bubble Meter

Rotameter

Lab Air Supply

Manometer
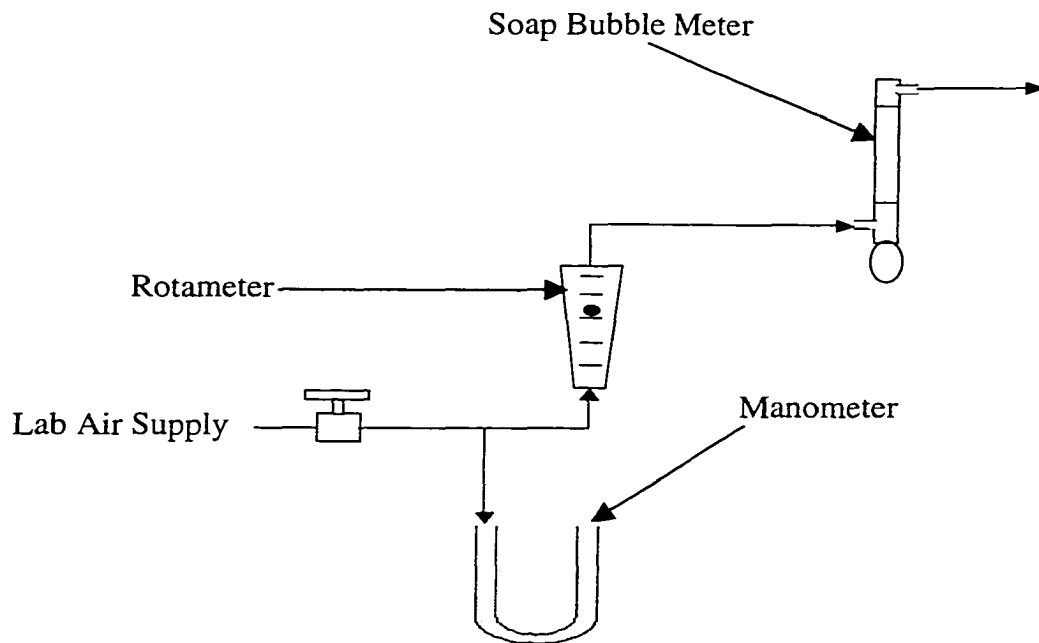
Figure B.3. Rotameter Calibration Setup

Figure B.4 and B.5 shows the calibration curves for the rotameter. Since the pressure drops across the rotameter (in the case of calibration experiments as well as

66

actual adsorption experiments) were very small (less than 1 psi), correction factors for changes in pressure were not applied.

Figure B.4. Rotameter Calibration (Flow Range 0 –1.5 L/min) using Soap Bubble Meter

Figure B.5. Rotameter Calibration (Flow Range 0 –5.6 L/min)

67

APPENDIX C

GC CALIBRATION

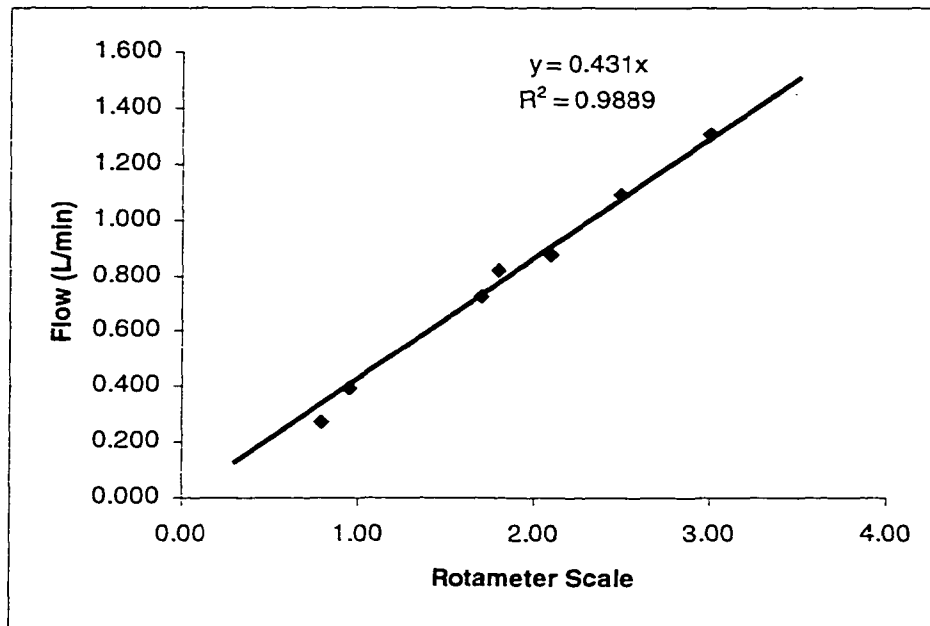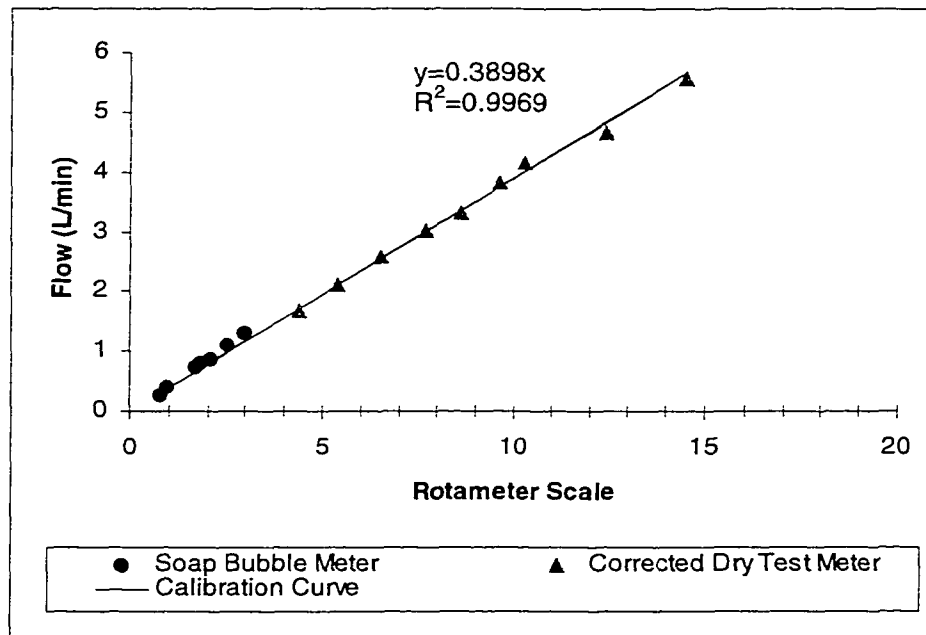The calibration of the GC/FID was needed to identify the retention time of m-xylene and to calculate unknown concentrations of m-xylene from instrument responses. Standards were prepared in tetrahydrofuran (THF) solvent in 10 mL volumetric flasks. The calibration was done using a range of approximately 0 to 1000 ppm liquid phase concentration. One micro-litre of sample was manually taken from each standard one at a time, and injected into the GC using a 10μL syringe. Three trials were performed for each standard. Linear regression analysis was applied to correlate the liquid phase concentration to the mean of the area responses. The standards were sampled from lowest to highest concentration to avoid cross contamination. Figure C.1 shows the calibration curve for m-xylene in the liquid phase.
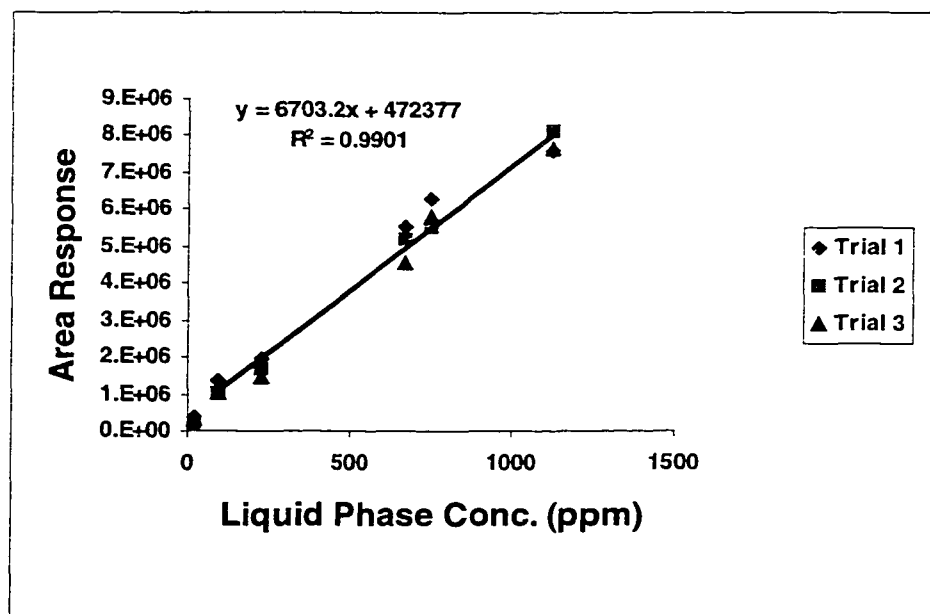

Figure C.1 GC Calibration of m-xylene (Liquid Phase)

68

To find the unknown concentrations in the vapor phase (in actual adsorption experiments) the calibration curve of Figure C.1 was transformed into Figure C.2 using a mass balance considering sampling volumes and densities in both the phases.

Sample Calculation:

Concentration of m-xylene in vapor phase: 1000 ppm

Sampling volume (vapor phase):   250 μL

Sampling volume (liquid phase):   1 μL

Hence, at 1 atmospheric pressure and 25° C

Volume of xylene in 250 μL vapor: 2.5×10^{-7} L

Mass of Xylene in 250 μL vapor: 1.0855×10^{-6} gm

Hence, in the liquid phase 1.0855×10^{-6} gm of m-xylene is required in 1 μL to have identical instrument responses to xylene in both the phases. This corresponds to 1262 ppm of m-xylene in the liquid phase (density at 25° C = 0.86 g/cc). Therefore, 1000 ppm m-xylene in the vapor phase $\equiv$ 1262 ppm m-xylene in the liquid phase.
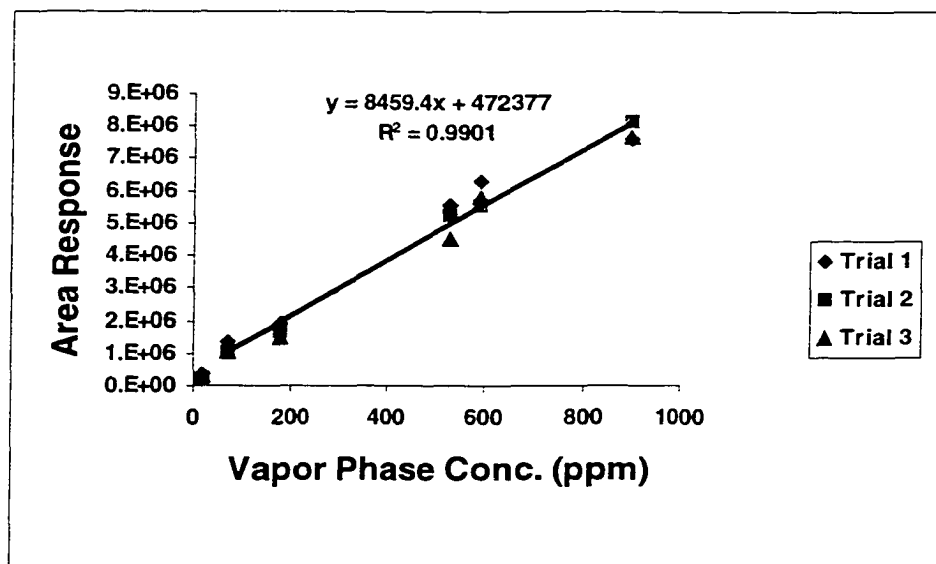
Figure C.2 GC Calibration of m-xylene (Vapor Phase)

69

For quality control the Means Chart for two of the standards (143.8 and 545.9 ppm) were constructed from the average and standard deviation of the values observed during calibration. This chart includes upper and lower warning levels (WL) and upper and lower control levels (CL). For the WL and CL construction, $\pm 2s$ and $\pm 3s$ limits were used respectively, where s represents standard deviation.

Figure C.3 Means Chart (C = 143.8 ppm)

Figure C.4 Means Chart (C = 545.9 ppm)

70

GLOSSARY

Activated Carbon   It is a highly porous, carbonaceous material. The very large porosity provides a large surface area, which results in exceptional adsorptive properties.

Adsorption   When a gas (or vapor) is allowed to come to equilibrium with a solid (or liquid) surface, the concentration of gas molecules is always found to be greater in the immediate vicinity of the surface than in the free gas-phase, regardless of the nature of the gas or surface. The process by which this surfa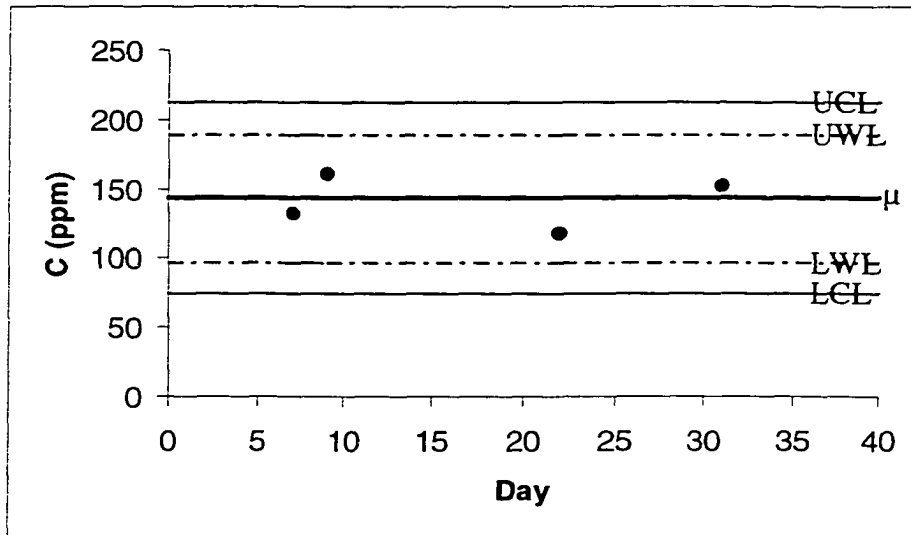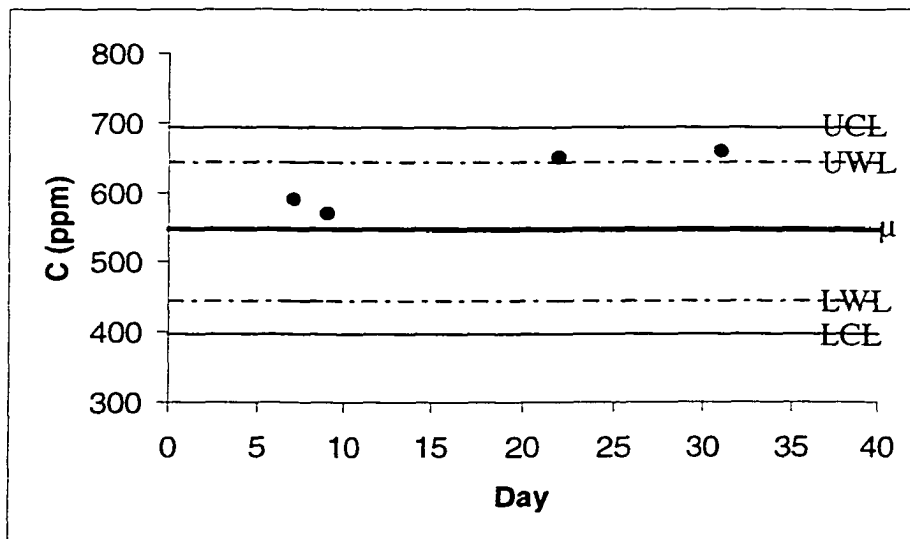ce excess is formed is termed adsorption (Young et al., 1962). The adsorbing phase is called **adsorbent**, and any substance being adsorbed is termed as an **adsorbate**.

BPL   It is a bituminous coal based virgin granular carbon activated at a high temperature in a steam atmosphere, designed for use in gas-phase applications.

Breakthrough Curve   The main feature of the dynamic behavior of fixed-bed adsorption is the history of effluent concentration. The concentration-time curve (or its equivalent) is commonly referred to as the breakthrough curve, and the time at which the effluent concentration reaches a threshold value is called the breakthrough time.

Brunauer Classification   Brunauer, Deming, Deming and Teller in 1940 divided the isotherms for physical adsorption into five classes (type I to type V). The isotherms for true microporous adsorbents, in which the pore size is not very much greater than the molecular diameter of the adsorbate molecule, are normally of type I. Isotherms of types II and III are generally observed only in adsorbents in which there is a wide range of pore

71

sizes (Ruthven 1984). Types IV and V are characteristic of multilayer adsorption on highly porous adsorbents, the flattening of the isotherms at the highest pressures being attributed to capillary phenomena (Young et al. 1962).

Capillary Condensation   In a porous adsorbent there is a continuous progression from multilayer adsorption to capillary condensation in which the smaller pores become completely filled with liquid adsorbate. This occurs because the saturation vapor pressure in a small pore is reduced, in accordance with the Kelvin equation, by the effect of surface tension (Ruthven et al. 1984).

Dispersion Force   This force originates through the rapidly changing electron density in one atom, which induces a corresponding electrical moment in a near neighbour, and so leads to attraction between the two atoms. Dispersion forces are always present in physical adsorption and unless the adsorbate molecule possesses a strong dipole moment, they will represent the major contribution to the total energy of adsorption.

Hazardous Air Pollutant   HAP is any air pollutant listed pursuant to section 122 (b) of 1990 amendments of Clean Air Act.

Isotherm   It is the relationship between the amount adsorbed and the pressure, for a given adsorbate on a given adsorbent at a fixed temperature (Gregg et al. 1967).

Micro-Pore   Based on the characteristic adsorptive behavior, Dubinin et al. (1975) classified the pore sizes (width of the pores) into macro, meso and micro pores. The equivalent radii of the smallest pore variety -micropores- are less than 6-7 Å.

72

Ozone Nonattainment Areas   These are the areas in the United States, which exceed the Ozone National Ambient Air Quality Standards (NAAQS). According to a *USA Today* computer Analysis, the ruling of the EPA July 1997 increased the total number of counties in the US in ozone nonattainment areas from 106 to more than 250 (Hussey et al. 1998).

Surface Diffusion   The rate of adsorption in porous adsorbents is generally controlled by transport within the pore network. It is convenient to consider intraparticle transport as a diffusive process and to correlate kinetic data in terms of diffusivity defined in accordance with Fick's first law of diffusion. Transport by movement of molecules over a surface is known as surface diffusion (Noll et al. 1992).

Volatile Organic Compound   VOC is any compound that contains carbon, excluding carbon monoxide, carbon dioxide, carbonic acid, metallic carbides or carbonates, and ammonium carbonate, which participates in atmospheric photochemical (smog formation) reactions (EPA's definition codified at 40 CFR 51.100(s)). A vapor pressure greater than 0.13 kPa is conventionally used to distinguish them from others (Bloemen et al. 1993).

REFERENCES

Adamson, A. W., and Gast, A. P. (1997). *Physical chemistry of surfaces*. John Wiley & Sons, Inc, New York.

ASTM (1995). *Standard guide for gas-phase adsorption testing of activated carbon.* American Society of Testing and Materials (D 5160 – 95).

Ayer, J. (1997). "Controlling VOC and air toxic emissions from aircraft refinishing facilities- a new approach." *The Air and Waste Management Association's 90th Annual Meeting and Exhibition, Toronto, Canada.*

Bailey, J. M. (1994). "Air force clears the sky." *Industrial Paint & Powder*, 12, 22-24.

Barton, S. S., Evans, M. J. B., and MacDonald, J. A. F. (1991). "The adsorption of water vapor by porous carbon." *Carbon*, 29(8), 1099-1105.

Barton, S. S., Evans, M. J. B., and MacDonald, J. A. F. (1992). "An equation describing water vapour adsorption on porous carbon." *Carbon*, 30(1), 123-124.

Basu, S., Henshaw, P. F., and N. Biswas. (2000). "Perspectives of adsorption in the new millennium", *The Environmental Specialty Conference, CSCE, London, Canada.*

Biron, E., and Evans, M. J. B. (1998). "Dynamic adsorption of water-soluble and insoluble vapours on activated carbon." *Carbon*, 36(7-8), 1191-1197.

Bloemen H. J. Th. and Burn, J. (1993). *Chemistry and analysis of volatile organic compounds in the environment.* Blackie Academic and Professional, Glasgow, UK.

Cal, M. P., Rood, M. J., and Larson, S. M. (1996). "Removal of VOCs from humidified gas streams using activated carbon cloth." *Gas Separation Purification*, 10(2), 117-121.

Carrott, P. J. M. (1995). "Molecular sieve behavior of activated carbons." *Carbon*, 33 (9), 1307-1312.

CCOHS (1984). *Chemical hazard summary - Xylene.* Canadian Centre for Occupational Health and Safety (Cat. No. CC273-4/84-3E).

Chou, M., and Chiou, J. (1997). "Modeling effects of moisture on adsorption capacity of activated carbon for VOCs." *Journal of Environmental Engineering, ASCE*, 123(5), 437-443.

Crittenden, J. C., Rigg, T. J., Perram, D. L., Tang, S. R., and Hand, D. W. (1989). "Predicting gas-phase adsorption equilibria of volatile organics and humidity." *Journal of Environmental Engineering, ASCE*, 115(3), 560-573.

DataFit, version 7.0, Oakdale Engineering, PA, 1995-2000.

Delage, F., Pré, P., and Cloirec, P. L. (1999). "Effects of moisture on warming of activated carbon bed during VOC adsorption." *Journal of Environmental Engineering, ASCE,* 125(12), 1160-1167.

Doong, S. J., and Yang, R. T. (1987). "Adsorption of mixtures of water vapor and hydrocarbons by activated carbon beds: thermodynamic model for adsorption equilibrium and adsorber dynamics." *Recent progress in adsorption and ion exchange,* Y. H. Ma and J. P. Ausikaitis, eds., AIChE, Symp. Ser. No. 259, 83, 87-97.

Dubinin, M. M., and Astakhov, V. V. (1971). "Description of adsorption equilibria of vapors on zeolites over wide ranges of temperature and pressure." *Advances in Chemistry Series,* R. F. Gould, Ed., vol. 102, 69-85.

Dubinin, M. M. (1975). "Physical adsorption of gases and vapors in micropores." *Progress in Surface and Membrane Science,* D. A. Cadenhead, et al., Eds., vol. 9, 1-70.

Dubinin, M. M. (1980). "Water adsorption and the microporous structures of carbonanceous adsorbents." *Carbon,* 18, 355-364.

Dubinin, M. M., and Serpinsky, V. V. (1981). "Isotherm equation for water vapor adsorption by microporous carbonaceous adsorbents." *Carbon,* 19(5), 402-403.

EPA (1995). *Survey of control technologies for low concentration organic vapor gas streams.* Control Technology Centre, Environmental Protection Agency (EPA-456/R-95-003).

Foley, N. J., Thomas, K. M., Forshaw, P. L., Stanton, D. and Norman, P. R. (1997). "Kinetics of water vapor adsorption on activated carbon." *Langmuir,* 13, 2083-2089.

Geffen, C. A. et al. (1998). "Economic and environmental tradeoffs in new automotive painting technologies." *SAE Technical Paper Series,* Paper No. 981164, 1-8.

Golovoy, A., and Braslaw, J. (1981). "Adsorption of automotive paint solvents on activated carbon: I. Equilibrium adsorption of single vapors." *Journal of the Air Pollution Control Association,* 31(8), 861-865.

Gong, R., and Keener, T. C. (1993). "A qualitative analysis of the effects of water vapor on multi-component vapor-phase carbon adsorption." *Journal of Air Waste Management Association,* 43, 864-872.

Grant, R. J., Joyce, R. S., and Urbanic, J. E. (1984). "The effect of relative humidity on the adsorption of water-immiscible organic vapors on activated carbon." *Fundamentals of*

Adsorption, Proeedings,of the Engineering Foundation Conference, Eds. A. L. Myers and G. Belfort), Bavaria, West Germany, 28, 316-333.

Gregg, S. J., and Sing, K. S. W. (1967). *Adsorption, surface area and porosity*. Academic Press.

Hall, T., Breysse, P., Corn, M. and Jonas, L. A. (1988). "Effects of adsorbed water vapor on the adsorption rate constant and the kinetic adsorption capacity of the Wheeler Kinetic Model." *American Industrial Hygiene Association Journal*, 49(9), 461-465.

Harsch, M., Finkbeiner, M., Piwowarczyk, D., and Saur, K. (1999). "Life-cycle simulation of automotive painting processes." *Automotive Engineering International*, February 1999, 211-214.

Hassan, N. M., Ghosh, T. K., Hines, A. L., and Loyalka, S. K. (1991). "Adsorption of water vapor on BPL activated carbon." *Carbon*, 29(4/5), 681-683.

Healey, M. J., Walsh, M. S., Kretkowski, D., and Lewis, J. (1998). "Industrial pollution prevention." *Odor and VOC control handbook*, H. J. Rafson, Editor in Chief, McGraw-Hill, New York.

Hellwig, G. V. (1998). "U.S. federal and state laws." *Odor and VOC control handbook*, H. J. Rafson, Editor in Chief, McGraw-Hill, New York.

Huggahalli, M., and Fair, J. R. (1996). "Prediction of equilibrium adsorption of water onto activated carbon." *Industrial Engineering Chemistry Research*, 35, 2071-2074.

Hussey, F., and Gupta, A. (1998). "Meet VOC regs with the right adsorbent." *Industrial Paint & Powder*, 3, 46-50.

Jonas, A. L., Sansone, E. B., and Farris, T. S. (1985). "The effect of moisture on the adsorption of chloroform by activated carbon." *American Industrial Hygiene Association Journal*, 46(1), 20-23.

Kawar, K. H., and Underhill, D. W. (1999). "Effect of relative humidity on the adsorption of selected water-miscible organic vapors by activated carbon." *American Industrial Hygiene Association Journal*, 60, 730-736.

Keener, T. C., and Zhou, D. (1990). "Prediction of activated carbon adsorption performance under high relativity conditions." *Environmental Progress*, 9(1), 40-46.

Khan, A. R., Ataullah, R., and Al-Haddad, A. (1999). "Equilibrium gaseous adsorption at different temperatures." *Journal of Environmental Engineering, ASCE*, 125(6), 548-555.

Kim, B. R. (1991). "Automotive wastes." *Research Journal WPCF*, 63(4), 486-489.

Kim, B. R., Kalis, E. M., Salmeen, I. T., Kruse, C. W., Demir, I., Carlson, S. L. and Rostam-Abadi, M. (1996). "Evaluating paint-sludge chars for adsorption of selected paint solvents." *Journal of Environmental Engineering, ASCE*, 122(6), 532-539.

Kim, B. R., Podsiadlik, D. H., Yeh, D. H., Salmeen, I. T. and Briggs, L. M. (1997). "Evaluating the conversion of an automotive paint spray-booth scrubber to an activated-sludge system for removing paint volatile organic compounds from air." *Water Environment Research*, 69(7), 1211-1221.

Kim, B. R., Kalis, E. M., DeWulf, T. and Andrews, K. M. (2000). "Henry's law constants for paint solvents and their implications on volatile organic compound emissions from automotive painting." *Water Environment Research*, 72(1), 65-74.

Kisarov, V. M. (1984). "Isotherm equation for the adsorption of water on carbon adsorbents." *Russian Journal of Physical Chemistry*, 58(8), 1203-1206.

Lin, T., and Nazaroff, W. W. (1996). "Transport and sorption of water vapor in activated carbon." *Journal of Environmental Engineering, ASCE*, 122(3), 176-182.

Lodewyckx, P., and Vansant, E. F. (1997). "The dynamic adsorption of water vapour on activated carbon." *Carbon*, 35(2), 310-311.

Lodewyckx, P., and Vansant, E. F. (1998). "The dynamic adsorption of water vapour on activated carbon." *Carbon*, 36(3), 304.

Lodewyckx, P., and Vansant, E. E. (1999). "Influence of humidity on adsorption capacity from the Wheeler-Jonas model for prediction of breakthrough times of water immiscible organic vapors on activated carbon beds." *American Industrial Hygiene Association Journal*, 60, 612-617.

Mancina, A. S. (1998). *"Achieving VOC reductions through pollution prevention & waste minimization."* Waste Reduction '98.

Manes, M. (1984). "Estimation of the effects of humidity on the adsorption onto activated carbon of the vapors of water-immiscible organic liquids." *Fundamentals of Adsorption, Proeedings, of the Engineering Foundation Conference*, Eds. A. L. Myers and G. Belfort), Bavaria, West Germany, 28, 316-333.

Moyer, E. S. (1983). "Review of influential factors affecting the performance of organic vapor air-purifying respirator cartridges." *American Industrial Hygiene Association Journal*, 44(1), 46-51.

Nelson, G. O. (1971). *Controlled test atmospheres – principles and techniques*. Ann Arbor Science Publishers, Inc.

Nelson, G. O., Correia, A. N., and Harder, C. A. (1976). "Respirator cartridge efficiency studies: VII. effect of relative humidity and temperature." *American Industrial Hygiene Association Journal*, 280-288.

Noll, K. E., Gounaris, V. and Hou, W. (1991). *Adsorption Technology for Air and Water Pollution Control*. Lewis Publishers, Inc., Michigan.

Okazaki, M., Tamon, H., and Toei, R. (1978). "Prediction of binary adsorption equilibria of solvent and water vapor on activated carbon." *Journal of Chemical Engineering of Japan*, 11(3), 209-215.

OSHA (1993). *"In-depth survey report: control technology for autobody repair and painting shops at Jeff Wyler Autobody Shop, Batavia, Ohio."* Report No. ECTB 179-15a.

Qi, S., Hay, K. J., and Rood, M. J. (1998). "Isotherm equation for water vapor adsorption onto activated carbon." *Journal of Environmental Engineering, ASCE*, 124(11), 1130-1134.

Qi, S., Hay, K. J., Rood, M. J., and Cal, M. P. (2000). "Equilibrium and heat of adsorption for water vapor and activated carbon." *Journal of Environmental Engineering, ASCE*, 126(3), 267-271.

Reid, R. C. Prausnitz, J. M., and Sherwood, T. K. (1977). *The properties of gases and liquids*. McGraw-Hill Book Company.

Riddick, J. A., Bunger, W. B., Sakano, T. K. (1986). *Organic solvents – physical principles and methods of purification*. John Wiley & Sons.

Rix, M. (1998). "Odor and VOC regulations in Canada." *Odor and VOC control handbook*, H. J. Rafson, Editor in Chief, McGraw-Hill, New York.

Rudisill, E. N., Hacskaylo, J. J., and LeVan, M. D. (1992). "Coadsorption of hydrocarbons and water on BPL activated carbon." *Industrial Engineering Chemistry Research*, 31(4), 1122-1130.

Rudzinski, W., and Everett, D. H. (1992). *Adsorption of gases on heterogeneous surfaces*. Academic Press Inc., CA.

Ruhl, M. J. (1993). "Recover VOCs via Adsorption on Activated Carbon", *Chemical Engineering Progress*, 89(7), 37-41.

Ruthven, D. M. (1984). *Principles of adsorption and adsorption processes*. John Wiley & Sons.

Spivey, J. J. (1988). "Recovery of volatile organics from small industrial sources." *Environmental Progress*, 7(1), 31-40.

Tien, C. (1994). *Adsorption calculations and modeling*. Butterworth-Heinemann, Boston.

Triplett, T. (1995a). "Emissions-reduction options for painting operations." *Industrial Paint & Powder* (http://www.ippmagazine.com).

Triplett, T. (1995b). "The waterborne dilemma." *Industrial Paint & Powder* (http://www.ippmagazine.com).

Werner, M. D. (1985). "The effects of relative humidity on the vapor phase adsorption of tricholoroethylene by activated carbon." *American Industrial Hygiene Association Journal*, 46(10), 585-590.

Werner, M. D., and Winters, N. L. (1988). "A review of models developed to predict gaseous phase activated carbon adsorption of organic compounds." *CRC Critical Reviews in Environmental Control*, 16(4), 327-356.

Young, D. M., and Crowell, A. D. (1962). *Physical adsorption of gases*. Butterworths, London.

VITA AUCTORIS

NAME   Sukanta Basu

PLACE OF BIRTH   Calcutta, India

YEAR OF BIRTH   1975

EDUCATION   Hindu School, Calcutta, India
                        1982-1994

                        Indian Institute of Technology, Kharagpur, India
                        1994-1998 B.Tech (Hons.) (Civil Engineering)

                        University of Windsor, Ontario, Canada
                        1999-2000 M.A.Sc (Environmental Engineering)